

## **Distribution Agreement**

In presenting this thesis or dissertation as a partial fulfillment of the requirements for an advanced degree from Emory University, I hereby grant to Emory University and its agents the non-exclusive license to archive, make accessible, and display my thesis or dissertation in whole or in part in all forms of media, now or hereafter known, including display on the world wide web. I understand that I may select some access restrictions as part of the online submission of this thesis or dissertation. I retain all ownership rights to the copyright of the thesis or dissertation. I also retain the right to use in future works (such as articles or books) all or part of this thesis or dissertation.

Signature:

---

Kevin E. Watkins

Date

**The effect of spinal cord injury on C-fiber low-threshold mechanoreceptors and sensory afferents that transiently express tyrosine hydroxylase**

By

Kevin E. Watkins  
Master of Science

Graduate Division of Biological and Biomedical Sciences  
Neuroscience

---

Dr. Shawn Hochman  
Advisor

---

Dr. Sandra Garraway  
Committee Member

---

Dr. Arthur English  
Committee Member

Accepted:

---

Lisa A. Tedesco, Ph.D.  
Dean of the James T. Laney School of Graduate Studies

---

Date

**The effect of spinal cord injury on C-fiber low-threshold mechanoreceptors and sensory afferents that transiently express tyrosine hydroxylase**

By

Kevin E. Watkins  
B.A., Dartmouth College, 2004

Advisor: Shawn Hochman, Ph.D.

An abstract of  
a thesis submitted to the Faculty of the  
James T. Laney School of Graduate Studies of Emory University  
in partial fulfillment of the requirements for the degree of  
Master of Science  
Graduate Division of Biological and Biomedical Sciences, Neuroscience  
2018

## Abstract

The effect of spinal cord injury on C-fiber low-threshold mechanoreceptors and sensory afferents that transiently express tyrosine hydroxylase

By Kevin E. Watkins

Chronic pain after spinal cord injury (SCI) greatly decreases the patient's quality of life, and complementary interventions addressing neural changes in the periphery have the potential to improve the often suboptimal present treatments. Allodynia is a common at-level pain syndrome in which normally innocuous stimuli are perceived as painful, and C-fiber low-threshold mechanoreceptors (C-LTMRs) have been implicated in mediating this neuropathic pain. Tyrosine hydroxylase (TH) has previously been identified as a genetic marker for C-LTMRs. In this study, a transgenic mouse strain expressing Cre recombinase in the tyrosine hydroxylase promoter sequence (TH-Cre) was crossed with a strain containing a Cre-dependent channelrhodopsin fused to a yellow fluorescent protein (ChR2-YFP). The offspring (TH::ChR2-YFP) express the light-activated ChR2 ion channel in a subset of TH-expressing (TH+) neurons, allowing for the recruitment of TH+ C-LTMR action potentials by shining blue light on the skin. I used these animals to pursue two goals: (a) confirm the recruitment of TH+ C-LTMRs and assess if they are selectively recruited by optogenetic stimuli; and (b) characterize changes in C-LTMR activity and physiology after SCI at and above the level of the injury. I found that TH::ChR2-YFP animals do express the transgene in TH+ C-LTMRs and those sensory neurons can be recruited by cutaneously applied blue light stimuli. Additional myelinated and perhaps unmyelinated neurons also express ChR2 and respond to light stimuli, possibly due to transient developmental expression of TH. I also found evidence that hemisection SCI caused a change in axonal membrane physiology of TH::ChR2-YFP C-fibers one spinal segment above the level of injury, shown by a change in action potential rise slope and peak amplitude. Furthermore, SCI caused a significant decrease in TH::ChR2-YFP sensory neuron activity at the level of injury, including the TH+ C-LTMRs. To our knowledge, this study is the first to identify changes in C-LTMR activity and physiology in response to SCI. These results may help to elucidate the peripheral changes that lead to SCI-induced at-level allodynia.

**The effect of spinal cord injury on C-fiber low-threshold mechanoreceptors and sensory afferents that transiently express tyrosine hydroxylase**

By

Kevin E. Watkins  
B.A., Dartmouth College, 2004

Advisor: Shawn Hochman, Ph.D.

A thesis submitted to the Faculty of the  
James T. Laney School of Graduate Studies of Emory University  
in partial fulfillment of the requirements for the degree of  
Master of Science  
Graduate Division of Biological and Biomedical Sciences, Neuroscience  
2018

## **Acknowledgments**

To my advisor, Dr. Shawn Hochman: thank you for believing in me, holding me accountable, helping me navigate my shortcomings, and appreciating me as an individual. I feel incredibly honored to have made this journey under your warm mentorship and friendship.

To my thesis committee, Drs. Sandra Garraway and Art English: thank you for your enthusiastic support, your smiles and laughter, and showing me what collaborative science can accomplish.

To Michael Sawchuk: thank you for the immense amount of time you invested in my training, always being willing to answer my many questions, and establishing the lab atmosphere that added so much to my experience.

To the present and former members of the Hochman, Garraway, and Alvarez labs, with particular thanks to Dr. Jacob Shreckengost, Dr. Don Noble, Michael McKinnon, Karmarcha Martin, Mallika Halder, Ruby Lam, Dr. Francisco Alvarez, Dr. Ron Griffith, Dr. Travis Rotterman, and Iris Spiegel: your help, expertise, and friendship were invaluable.

To the Emory Neuroscience Program students, especially the class of 2011: thank you for being like a family and for the privilege of serving as a representative on committees and during recruitment. Thank you for the late nights, the interesting conversations, the study sessions, the chance to be in a jug band, and the camaraderie.

To my undergraduate teaching mentors, Drs. Leah Roesch and Pat Marsteller: thank you for helping me continue developing my skills as an educator to better ignite the passion for science in others.

To the Emory Neuroscience Program faculty leadership, especially Drs. Malu Tansey and Victor Faundez: thank you for truly caring about the NS students and going above and beyond in supporting us in every way imaginable.

To Dr. Lisa Parr: thank you for taking a chance on me, seeing my determination, believing in me when few others did, and allowing me the opportunity to live my dream of designing and implementing a behavioral experiment on the wonderful chimpanzees at Yerkes.

To my undergraduate students and volunteers, Loris Takori and Lucy Galvin: thank you for your help with this research. I am so lucky to have been able to work with you.

Most of all, to my wife, Laura: thank you for your love, support, and understanding throughout this long process. Thank you for believing in me, especially when I found it hard to believe in myself.

This research project was supported in part by the Department of Defense Spinal Cord Injury Research Program grant awarded to Dr. Sandra Garraway (SC140210) and the NIGMS-funded Neuroscience Training grant.

## Table of Contents

### **Introduction**

Allodynia in patients with spinal cord injury.....	1
Traits of C-fiber low threshold mechanoreceptors (C-LTMRs).....	2
C-LTMR processing in the dorsal horn and implications for allodynia.....	3
Evaluating changes in C-LTMR activity after SCI.....	5

### **Method of Approach**

Animal subjects.....	9
Experimental methods.....	11
Analysis methods.....	15

### **Results**

Anatomy of TH::ChR2-YFP.....	19
Electrophysiology of TH::ChR2-YFP.....	22
Action potential properties were different between ChR2-YFP+ units contralateral and ipsilateral to SCI.....	26
Dermatome mapping revealed significant changes in T10 DCN activity.....	28

### **Discussion**

Evaluating the Tg(Th-cre)1Tmd driver for transgene expression in DRG neurons.....	33
Effects of SCI on TH::ChR2-YFP cutaneous neurons.....	38

<b>Conclusion</b> .....	43
-------------------------	----

<b>References</b> .....	46
-------------------------	----

### **Figures and Tables**

Table 1: Distribution of animal subjects	9
Figure 1: Dorsal root ganglia neurons from TH::ChR2-YFP mice	19
Figure 2: TH and ChR2-YFP expression in dorsal cutaneous nerves	20
Figure 3: TH::lacZ cutaneous end organ $\beta$ -gal staining	20
Figure 4: Central projections of TH::ChR2-YFP neurons	21
Figure 5: Example DCN recordings of optogenetic response	23
Table 2: Action potential properties of TH::ChR2-YFP neurons in DCN	24
Figure 6: Responses to von Frey hair stimuli	24
Figure 7: Responses to mechanical brush	25
Table 3: Action potential measurements after SCI	27
Figure 8: Comparison of action potential properties after SCI	28
Figure 9: Dermatome area maps	31
Figure 10: DCN ipsilateral vs. contralateral relative intensity maps	32

## Introduction

### **Allodynia in patients with spinal cord injury:**

A majority of spinal cord injury (SCI) patients suffer from chronic pain, which interferes with rehabilitation, daily activities, and quality of life (Siddall *et al.*, 2003). Allodynia is a common feature of chronic SCI neuropathic pain and is defined as a painful response to normally innocuous stimuli. People with tactile allodynia typically experience a tender, burning sensation when the affected skin is stroked softly (Rasmussen *et al.*, 2004). Conversion of the sensation of a loved one's gentle caress to a sensation of pain would be a particularly poignant example of allodynia. While loss of motor function is a primary focus of spinal cord injury (SCI) research, chronic pain syndromes – including neuropathic, visceral, and musculoskeletal pain – decrease quality of life so severely that depression and suicide frequently result (Christensen and Hulsebosch, 1997; Cairns, Adkins, and Scott, 1996; Segatore, 1994). While basic research has helped uncover many of the central mechanisms underlying neuropathic pain, therapeutic interventions are often suboptimal or ineffective and highly understudied in relation to SCI. A better understanding of how peripheral sensation changes after SCI could help to improve the therapeutic interventions currently available.

Neuropathic pain after SCI may occur above, at, or below the level of lesion and may persist for years after the acute injury (Calmels, Mick, Perrouin-Verbe, and Ventura, 2009). Pain progresses from at- to below-level pain, possibly due to interactive mechanisms between these two conditions (Siddall *et al.*, 2003). The development of allodynia is an important feature of at-level pain, specifically. Clinical observations of

SCI patients with ongoing pain have shown that gentle brush stimuli provided to at-level hairy skin dermatomes, normally perceived as pleasant, produces allodynia in these patients (Finnerup *et al.*, 2003). This type of gentle brush stimulation is known to preferentially recruit a specific population of unmyelinated sensory afferents, the C-fiber low threshold mechanoreceptors (C-LTMRs) (Iggo, 1960).

### **Traits of C-fiber low threshold mechanoreceptors (C-LTMRs):**

In uninjured conditions, C-LTMRs (called CT afferents in the human literature) are tuned to encode pleasurable touch information to the point that firing rates correlate significantly with stimulus pleasantness ratings (Nordin, 1990; Löken *et al.*, 2009). Though C-LTMRs react to the same stimuli as myelinated fibers (A $\delta$ - and A $\beta$ -LTMRs), they show unique activation curves tuned to innocuous tactile stimulation. Human forearm C-LTMR firing frequencies form an inverted U-shaped relationship with brush stimulus velocity, and velocities between 1-10 cm s<sup>-1</sup> evoke peak responses (Löken *et al.*, 2009). Myelinated afferents, conversely, show either a linear or positive quadratic relationship between brush velocity and firing rates (Löken *et al.*, 2009). Also, studies from humans and mice show that C-LTMRs are slow conducting afferents (conduction velocities ranging from 0.6-1.2 m/s) and are recruited at low stimulation forces (<5 mN) (Li *et al.*, 2011; Bessou *et al.*, 1971; Seal *et al.*, 2009; Vallbo, Olausson, and Wessberg, 1999). These slow, seemingly redundant C-LTMRs comprise a second anatomically and functionally distinct system for signaling touch. Their preference for stroking stimuli and the central processing pathway for their signals differ from myelinated touch afferents, and these properties have resulted in researchers referring to them as the

emotional or affective touch system. While the fast myelinated mechanosensory pathway projects to somatosensory cortex (Blomqvist *et al.*, 2000), C-LTMRs relay information to the insula (Olausson *et al.*, 2002) – an area associated with allostatic control, motivation, and feelings (for reviews, see Paulus and Stein, 2006; Craig, 2008) – and recruit a network of brain regions involved in social processing (Gordon *et al.* 2013). The C-LTMRs have been hypothesized to play an integral part in the interoceptive C-fiber afferent network that gives rise to “gut feelings” (for review, see Björnsdotter, Morrison, and Olausson, 2010). Because of these traits, dysfunction in the sensation and processing of the C-LTMR-mediated affective touch system may also play an important role in the development of depression and other mood disorders arising after SCI.

### **C-LTMR processing in the dorsal horn and implications for allodynia:**

An understanding of global mechanisms producing SCI-induced allodynia is understandably complex due to do the heterogeneity and complexity of the injury itself (Yeziarski *et al.*, 2004). SCI can cause cellular changes in the central nervous system that alter the excitability of neurons in the spinal cord, particularly in the dorsal horn. This central sensitization is thought to result from elevated levels of neuronal activity, glutamatergic transmission, and glial activation (Watson *et al.*, 2014). Descending monoaminergic pathways are also thought to play a role, specifically facilitation by serotonergic mechanisms on 5-HT<sub>3</sub> receptors (Oatway, Chen, and Weaver, 2004).

Regarding the dorsal horn circuitry underlying allodynic pain states, research has progressed greatly in the past decade but has consistently revealed more complexity. In

the dorsal horn, C-LTMR axon terminals overlap with protein kinase C gamma (PKC $\gamma$ ) neurons in the inner ventral region of lamina II (I<sub>liv</sub>) of the dorsal horn (Li *et al.*, 2011), where they preferentially synapse with PKC $\gamma$ , Ror $\beta$ , and excitatory parvalbumin interneurons (Abraira *et al.*, 2017, but see Peirs *et al.*, 2014). From there, the recipient zone for low-threshold mechanosensation, which stretches from lamina I<sub>liv</sub> to lamina IV, is comprised almost completely of interneurons that receive input from local interneurons, 2-3 types of LTMR sensory afferents, and descending cortical inputs (Abraira *et al.*, 2017). This LTMR recipient zone likely performs initial processing of innocuous touch, similar to the processing of visual stimuli in the retina (Abraira *et al.*, 2017). C-LTMR activity is eventually transmitted via wide dynamic range NK1R+ lamina I spinoparabrachial projection neurons, which also transmit C-fiber nociceptive information (Andrew, 2010). Interestingly, Keller *et al.* (2007) found that an increased percentage of lamina I spinoparabrachial neurons responded to innocuous brush stimulation under conditions of nerve injury, and the mean response to that brush stimuli increased. C-LTMRs also influence information flow from C-fiber nociceptors to lamina I NK1R+ projection neurons through excitatory input on GABAergic islet cells in lamina II (Lu and Perl, 2003), and their PKC $\gamma$ + interneuron targets have been shown to mediate pain behaviors after peripheral nerve injury and inflammation (Malmberg, Chen, Tonegawa, and Basbaum, 1997). Two research groups recently described the dorsal horn inputs and interneuron circuitry that may be involved in converting innocuous touch to nociceptive signals, though much is still unknown (see Peirs and Seal, 2016; Koch, Acton, and Goulding, 2018). These results, along with the analgesic properties of C-LTMR-secreted TFAA4 (Delfini *et al.*, 2013) which is reduced during tactile allodynia

(Liljencrantz *et al.*, 2013), implicate the C-LTMRs in modulating allodynia and make them an important target for chronic pain research. To our knowledge, the contribution of C-LTMRs to pain hypersensitivity following SCI has not been directly studied.

### **Evaluating changes in C-LTMR activity after SCI**

A handful of genes have been proposed as markers for C-LTMRs in mouse models. One of the first put forward, Mas-related G protein-coupled receptor B4 (MrgprB4), is expressed in a small population (~2%) of thoracic DRG neurons (Liu *et al.*, 2007). MrgprB4+ neurons are responsive to massage-like stroking over a broad surface area in vivo but were not recruited in an *ex vivo* isolated skin-nerve preparation (Vrontou *et al.* 2013). They continue to be considered a separate and unique population of C-LTMR-like afferents that do not express the more recently proposed C-LTMR markers. Li *et al.* (2011) identified tyrosine hydroxylase (TH), the rate limiting enzyme in the production of catecholamines (Levitt, Spector, Sjoerdsma, and Udenfriend, 1965), as another purported marker of C-LTMRs. They comprise >15% of sensory ganglion neurons innervating the trunk hairy skin, selectively innervate lamina IIIV of the dorsal horn, arborize extensively, and form longitudinal lanceolate endings around hair follicles with zigzag and awl/auchene hairs (Li *et al.*, 2011). Despite their small sizes and lack of myelin, these touch afferents do not express the classic nociceptive neuropeptides (CGRP, TrpV1, and TrkA), nor do they bind the lectin IB4, further distinguishing them as non-nociceptors (Li *et al.*, 2011).

Two more purported markers of C-LTMRs appear to identify subsets of the TH+ C-LTMR group: vesicular glutamate transporter 3 (VGLUT3; Seal *et al.*, 2009) and TAF4A

(Delfini *et al.*, 2013). Myelinated VGLUT3+ neurons only express the gene transcript transiently during development, and unmyelinated VGLUT3+ neurons continue to express the protein in the adult. This second group, the VGLUT3-persistent neurons, show the response properties of classic C-LTMRs (Seal *et al.*, 2009) and can further be divided into TH+/VGLUT3+ (~67%) and TH-/VGLUT3+ (~33%) neurons (Lou *et al.*, 2013). It has also been reported that >80% of TH+ DRG neurons express VGLUT3 (Li *et al.*, 2011), though a more recent RNA sequencing study on 622 single neurons from the mouse lumbar DRGs found that 34% of TH+ neurons were VGLUT3+ and 93% of VGLUT3+ neurons were TH+ (Usoskin *et al.*, 2015). Most recently, Delfini *et al.* (2013) demonstrated TFAFA4, a chemokine-like secreted protein (Tom Tang *et al.*, 2004), also identified neurons with response properties and expression patterns of C-LTMRs and overlapped extensively with the VGLUT3+ population (92% VGLUT3+ are TFAFA4+ and 94% TFAFA4+ are VGLUT3+). They further demonstrated that TFAFA4 null mice showed sustained mechanical allodynia under conditions of inflammation and nerve injury, and this effect was reversed upon intrathecal administration of TFAFA4 protein (Delfini *et al.*, 2013). To summarize, C-LTMRs appear to be a heterogeneous group based on their expression profiles, with the largest group defined by the expression of TH.

To better characterize the role of C-LTMRs in allodynia, we developed a transgenic mouse model to selectively recruit C-LTMR afferents without simultaneously activating myelinated mechanoreceptors. We chose to use TH as our genetic marker for C-LTMRs based on published results showing it identifies the largest C-LTMR population (Li *et al.*, 2011; Delfini *et al.*, 2013; Usoskin *et al.*, 2015). Our model involves crossing transgenic mice expressing Cre recombinase in TH-expressing (TH+) neurons (TH-Cre) with mice

expressing a Cre-dependent fluorescent marker fused to a light-gated ion channel, channelrhodopsin 2 (ChR2-YFP). The resultant animals express the light-activated ChR2 in cells that express TH (TH::CHR2-YFP), allowing for optogenetic activation of TH+ C-LTMRs with cutaneously applied blue light. This TH-Cre driver strain has been shown to cause recombination of few to most of the TH+ neurons, depending on the structure, and recombination in cells that may express TH transiently during development has also been reported (Lindeberg *et al.*, 2004).

Using an *ex vivo* skin and nerve preparation to characterize the population of cutaneous afferents expressing ChR2-YFP in TH::ChR2-YFP mice, I recorded neural impulses from dorsal cutaneous nerves (DCNs) while the isolated dorsal thoracic skin received optogenetic and mechanical stimuli. Initial optogenetic identification of ChR2-YFP+ neurons was followed with calibrated von Frey stimulation and computer-controlled robotic brush stimulation at speeds of 0.3 to 55 cm s<sup>-1</sup>.

The second goal of this study was to determine if peripheral C-LTMR physiology may play a role in the transformation of normally pleasant tactile stimuli into painful stimuli during SCI-induced allodynia. This would identify a new chronic pain intervention target to improve outcomes for patients with allodynia. Using this preparation, I analyzed recordings of unitary C-LTMRs in peripheral nerves to characterize how SCI changes their recruitment properties – including receptive field size, conduction velocity, spike shape properties, and overall activity – at and above the thoracic segmental dermatomal site of lesion. I conducted DCN recordings from T9 and T10 segmental dermatomes in skin-nerve preparations from animals after level T10 hemisection SCI. In mice, injury at this level (T10/T11) is associated with behavioral deficits such as

impaired locomotor (Basso *et al.*, 2006; Jakeman *et al.*, 2006) and bladder function (David *et al.*, 2014) and the development of neuropathic pain (Murakami *et al.*, 2013). Recording and stimulating at segmental levels T9 and T10 allowed me to compare modifications in above- and at-lesion-level afferents after injury.

Though my mouse model recruited a heterogenous group of afferents, possibly due to transient TH expression in development (Lindeberg *et al.*, 2004; Jonakait *et al.*, 1984), we did recruit TH+ CLTMRs using optogenetic stimuli. In analyzing responses within C-fiber conduction velocity range, I found a significant decrease in levels of activity ipsilateral to SCI at the level of the lesion. Above the lesion, action potentials from TH::ChR2-YFP+ cutaneous neurons ipsilateral to injury showed increased peak amplitude and rise slope, though the T9 DCN dermatome as a whole apparently decreased in area. The results of this study identify key changes in peripheral TH+ afferents in response to hemisection SCI near the level of injury and has the potential to establish C-LTMRs as therapeutic intervention target for at-level allodynic pain states after SCI.

## Method of Approach

### Animal subjects:

All procedures were approved by the Institutional Animal Care and Use Committee of Emory University. Animals used in this study were transgenic and wild-type mice of a C57/Bl6 background, specifically B6.Cg-Tg(Th-cre)1Tmd/J (TH-Cre driver), Ai32D-ChR2-YFP (floxed stop-channelrhodopsin-yellow fluorescent protein), and R26-LacZ (lacZ). TH-Cre mice were crossed with each of the other strains to produce animals expressing the desired proteins in TH+ cells. The resultant subject mice expressed Cre-driven ChR2-YFP (n=20) and lacZ (n=1) (see Table 1).

### *Surgical procedures:*

For SCI procedure, adult mice (approximately 8-10 weeks old) were deeply anesthetized with isoflurane. A skin incision and dorsal laminectomy, under sterile conditions, exposed the spinal cord at T10. The spinal cord was hemisected at this location. The overlying muscle and skin were sutured, and mice were left to recover.

Sham control mice underwent the surgical procedure but did not receive a SCI. Dr. Sandra Garraway performed all surgical procedures.

**Table 1: Distribution of animal subjects.** A total of 21 mice were used in these experiments. Twenty TH::ChR-YFP mice were used, divided amongst treatments of SCI, sham SCI, and uninjured. Most of these mice underwent a combination of experiments. One TH::LacZ mouse was also used for histological staining.

Treatment	Protein expressed	Experiment
SCI	ChR-YFP (n=8)	Optogenetic characterization (n=7)
		Dermatome mapping (n=6)
		Low threshold stimulation (n=2)
		von Frey (n=4)
		Brush (n=2)
Sham SCI	ChR-YFP (n=2)	Imunohistochemistry (n=8)
		Optogenetic characterization (n=1)
		von Frey (n=1)
Uninjured	ChR2-YFP (n=10)	Dermatome mapping (n=1)
		Imunohistochemistry (n=2)
	lacZ (n=1)	Optogenetic characterization (n=2)
		Imunohistochemistry (n=8)
		Histology (n=1)

All electrophysiology experiments were acute *ex vivo* preparations. Mice were euthanized by carbon dioxide inhalation in accordance with IACUC protocols. Hair along the trunk and abdomen was removed by electric trimmers to allow for light penetration to the cutaneous surface, and an incision was made along the dorsal midline of the skin. The trunk skin on one side was dissected away by separating the skin from underlying connective tissue using blunt dissection, being careful not to injure the dorsal cutaneous nerves (DCNs). Recirculating oxygenated synthetic interstitial fluid (SIF; Bretag, 1969) was then added to the cavity between the ribcage and the skin and was refreshed periodically. Connective tissue around the DCNs was carefully removed, and DCNs T8-T11 were cut where they entered the musculature of the ribcage, leaving the proximal ends free-floating in SIF and the distal ends attached to the skin. A rectangular section of trunk skin containing the DCNs was then removed, extending rostrocaudally from the shoulder to the hip joint and from the dorsal midline to the ventral surface of the mouse. This section of skin was then placed in a static SIF-oxygenated bath. The dissection procedure was then repeated for the other side of the mouse. After both sides of the dorsal cutaneous surface were removed, the spinal column was dissected out and placed in 4% paraformaldehyde for 24-48 hours before being placed in 30% sucrose solution for later sectioning and immunohistochemistry procedures.

### **Experimental methods:**

One of the two skin sections was removed from the static SIF bath and placed in a recording chamber with the external surface facing up. The chamber contained circulating and oxygenated SIF maintained at a temperature of 34°C using a

temperature feedback controlled inline heater. Grooved channels in the base of the chamber allowed for SIF to circulate underneath the skin and reach the DCNs and subcutaneous surface while the epidermis remained dry. DCNs T8-T11 were gently drawn out from under the skin using light suction so that the free-floating proximal nerve endings extended beyond the dorsal midline. The preparation was then allowed to rest for 30 minutes to acclimate. DCNs T9 and T10 were then attached to constricted suction electrodes, where the opening of the glass pipette was larger than the minimum diameter of the suction electrode, similar to an open-ended hourglass. These electrodes were constructed and selected to allow for recording from the entire nerve while maintaining adequate suction throughout the recording session. If I was unable to elicit a response from the T9 or T10 DCN by mechanical and optogenetic stimuli, electrodes were then attached to the T8 or T11 DCN for recording.

Suction electrodes were connected to an in-house built differential amplifier with a gain of 1000, a Hum Bug™ Noise Eliminator (Quest Scientific, North Vancouver, BC, Canada), a Digidata1322A (Molecular Devices) and Dell XPS computer running LabView™, pClamp and ClampEX data acquisition software (Molecular Devices). The rig was also equipped with an in-house developed robotic stimulator device with attached brush and a computer-controlled 2W 445nm copper module laser with a 405-G-2 glass lens and fiber-optic cable. All elicited responses were recorded digitally for offline analysis (Clampfit, Molecular Devices).

#### *Optogenetic characterization of ChR2+ cutaneous neurons:*

We optogenetically activated cutaneous neurons in TH::ChR2-YFP mice using a laser providing blue light for optogenetic skin stimulation. A fiberoptic cable attached to

a micromanipulator with X-Y coordinate system, positioned 5 mm above and perpendicular to the skin, allowed for light to be focused on a circular region of the skin 1-2 mm in diameter. An Axon Instruments Digidata 1322A run by Clampex software controlled the frequency, duration, and intensity of the light stimulation. Light intensity of  $1.8 \text{ mWmm}^{-2}$  recruited robust firing of ChR2 cutaneous neurons in transgenic mice without causing responses from nerve terminals in control mice.

For dermatome mapping, the dermatomes of the recorded DCNs were roughly explored by scanning the cutaneous surface with the fiberoptic cable supplying blue light illumination. The fiberoptic cable was then positioned with the micromanipulator at the dorsal midline outside of the receptive field, and each square millimeter of the receptive field was systematically given a 10ms, 2 Hz pulse train applied for 2.5 seconds before the fiberoptic cable was moved.

For characterization of individual units, strategic light placement at nerve receptive field borders was used to aid in selective recruitment of individual neurons for subsequent analysis. When few individual units were found, a 2 Hz pulse train lasting three minutes, with 10 ms pulses, was applied to that location. After a rest period of three minutes, the same location received pulse trains of 10, 15, and 20 Hz in succession with a 10 second inter-stimulus interval.

#### *Mechanical stimulation:*

In selected trials, the area of illumination was subsequently tested to characterize optogenetically responsive units using calibrated Von Frey filaments which stimulate at forces 3.9, 5.9, 7.8, and 9.8 mN. First, baseline activity was recorded with no

mechanical stimulation. The filaments were then bent against the skin for about 2 to 3 seconds to deliver the desired force. Each force was administered repeatedly over a period of 30 seconds. C-LTMRs were identified by the firing threshold of 3.9 mN. Emphasis was on targeting already optogenetically-identified C-fiber neurons ( $CV < 1.2$  m/s) using coordinates provided in optogenetic experiments above.

In some animals, a computer controlled robotic arm administered brush strokes using a fine tipped artist's brush over areas of the receptive field in the direction of hair growth at brush speeds of 1, 3, 10, 30, and 55 cm/s. These speeds overlap with those shown to preferentially activate C-LTMRs in relation to other LTMRs (Li *et al.*, 2011; Seal *et al.*, 2009). Each speed was tested four times with an inter-stimulus interval of 30 seconds. Responses to each speed of brush were recorded and used for template searches, as described in Data Analysis section.

After the completion of all experiments, the lengths of the DCNs were measured, and the skin and attached DCNs were placed in 4% paraformaldehyde for 24 hours and then placed in 30% sucrose to preserve the tissue for later analysis.

#### *Immunohistochemistry:*

Mice not used in other experiments were deeply anesthetized with urethane (2 mg/kg), placed on ice, and transcardially perfused with heparinized saline followed by 4% paraformaldehyde in phosphate buffered saline. The spinal cord and attached dorsal root ganglia were then removed and placed in 4% paraformaldehyde overnight and then in 30% sucrose solution until ready for sectioning. For animals that underwent electrophysiological testing, the preserved spinal cord was isolated by carefully

removing the surrounding spinal tissue, and dorsal root ganglia were removed and sectioned separately.

A portion of the spinal cord from T8 to T12 was isolated and placed in a 1.5% agar gel block. This tissue was then sectioned to 50  $\mu\text{m}$  on a vibrating blade microtome (Leica VT1000S). Sections were collected serially in wells, and every fifth section was collected in the same well. Sections from the different spinal cord levels (T8-T11) were collected separately. Dorsal root ganglia were embedded in O.C.T. and sectioned to 25  $\mu\text{m}$  on an upright Leica cryostat. The sectioned tissue was mounted on slides for immunohistochemical procedures. DCNs were cut from the skin and placed in wells containing phosphate buffered saline (PBS).

Spinal cord sections and isolated DCNs were washed in 0.1% Triton X-100 in phosphate buffered saline PBS, pH 7.4, for two hours. Sheep polyclonal anti-TH (Millipore), guinea pig polyclonal anti- $\alpha\text{CGRP}$  (Peninsula), chicken polyclonal anti-GFP (Abcam), rabbit anti-PKC $\gamma$  (Santa Cruz Biotechnology), or rabbit anti-TrpV1 (Alomone Labs) were diluted in PBS and applied overnight. The GFP antibody also adheres to YFP and was used to amplify the ChR2-YFP signal. The following day, sections were washed three times, 30 minutes each, in 0.1% Triton PBS. Secondary antibodies Cy5 donkey anti sheep (Jackson immunoresearch 1:100), Cy5 donkey anti-rabbit (Jackson immunoresearch 1:100), Alexa 647 donkey anti-guinea pig (Jackson immunoresearch 1:100), Cy3 donkey anti-chicken (Jackson immunoresearch 1:250) were added and the tissue was incubated for 1.5 hours at room temperature. Spinal cord sections were then washed three times, 30 min each, and mounted to slides. DCNs were whole-mounted onto slides.

DRG sections on slides were washed for 2 hours in 0.1% Triton PBS at room temperature and incubated with the above antibodies overnight at 4°C. Slides were washed three times, 15 min each, in 0.3% Triton PBS. Secondary antibodies were added and the tissue was incubated for 1.5 hours at room temperature. Sections were then washed three times for 15 min each.

#### *LacZ staining:*

Cryostat sectioned thoracic spinal cord, DRG, and whole skin mounts were washed 3x 30 min in PBS-T at room temperature. Sections were incubated in LacZ rinse buffer (0.2 M Sodium Phosphate, 20mM Magnesium Chloride, 225 mM Sodium Deoxycholate, 0.02% IGEPAL630) for 2 hours at 37°C. Tissue was then incubated in LacZ staining solution (2ml LacZ rinse buffer, 5mM Potassium Ferrocyanide, 5mM Potassium Ferricyanide, 0.5mg/ml X-GAL) at 37°C for 4-24 hours.

#### **Analysis methods:**

##### *Electrophysiology*

Threshold detection in Clampfit was used to identify individual units responding to the 2 Hz optogenetic stimuli (10 ms pulses for 3 minutes). Each detected event was manually accepted or rejected for analysis based on visual inspection to reduce the effects of noise and artifacts on characterization of the action potential shapes.

Conduction velocity was calculated by dividing the measured DCN length by the time difference between the onset of light stimuli and the peak of the event. Descriptive

statistical analysis of events was carried out on Clampfit software to obtain means and standard deviations of amplitude, half-width, rise slope, and decay slope.

In cases where the same area of skin received both optogenetic and mechanical stimulation – by von Frey hairs or robotic brush – the identified action potentials from the 2 Hz optogenetic stimulation threshold detection search were used to create waveform templates for a template search of mechanical stimulation recordings. The peaks of the action potentials were aligned before creating an average trace. This average trace was then used as a template to search the robotic brush and von Frey hair recordings in Clampfit using a template match threshold value of 4 and 6-12, respectively. These conservative threshold values were selected for each template search in the mechanical stimulation recordings with an aim of minimizing detected events in the baseline traces while still retaining events in the experimental traces (for a description of the template match threshold, see Clements and Bekkers, 1997). Descriptive statistical analysis of instantaneous frequency data for these events was performed in Clampfit. Responses to robotic brush stimuli were grouped by brush speed and responses to von Frey stimulation were grouped by force.

For the receptive field heat maps, the level of response was defined as the integral of the absolute value of the signal. This produced the cumulative area between the signal and the baseline in the region of interest. For each square millimeter, two regions were selected for each of the five stimuli: an early response ( $CV > 1.2$  m/s) and a late response ( $CV < 1.2$  m/s). The responses to the five pulses of stimuli were averaged to get the mean response to optogenetic stimuli in that  $1 \text{ mm}^2$  of skin. This was repeated for every square millimeter of the dermatome recorded, for each nerve

recorded, and for each side of the skin (ipsilateral/contralateral). The individual receptive fields in the same nerve-and-side group were then centered in the rostrocaudal direction so that the most active pixel of each receptive field was aligned between individuals. The individual response means were then averaged across all samples in each group. For the dermatome average map, these means for each receptive field map were scaled to a range of 0-100 before averaging across animals and receptive field size was determined by counting the number of square millimeter regions containing responses above a scaled response of 50. This conservative threshold for inclusion was based on the observation that some dermatomes contained high scaled values in areas clearly outside of the receptive field. In the relative response intensity comparison maps, raw activity data for both ipsilateral and contralateral responses were scaled together before aligning and averaging across all individuals (i.e. each pair scaled together). Cells above the median were averaged to create a relative intensity mean response for statistical analysis.

#### *Immunohistochemistry:*

All tissues were viewed and photographed using an Olympus BX51 upright fluorescence microscope. DRGs of three mice were used to compare the relative sizes of neurons expressing ChR2-YFP, TH, and CGRP. The cross-sectional area of each immunolabeled neuron was calculated in the public domain NIH program ImageJ and plotted into histograms. The average size of ChR2-YFP+ and TH+ DRG neuron groups was calculated for statistical analysis.

*Statistical analyses:*

To compare the means between two groups, I first conducted a Levene's test for homogeneity of variances. Based on these results, I used either a Student's t-test (equal variances) or a Welch's t-test (unequal variances) to assess the significance of differences in the means. The Holm-Bonferroni method for multiple comparisons was used to adjust  $\alpha$  when comparing multiple action potential parameters between groups. For the comparison between axonal action potential properties in SCI animals, a two-way ANOVA was used to establish an effect of treatment before post-hoc paired t-tests comparing T9 ipsilateral to T9 contralateral and T9 ipsilateral to T10 ipsilateral.

## Results

### Anatomy:

To determine the specificity and extent of ChR2-YFP expression in TH+ C-LTMRs, I isolated the DRG neurons of thoracic spinal segments of 5 animals for immunohistochemical analysis. All DRG tissue was incubated with antibodies for GFP to amplify the signal. DRG tissue sections from four animals were also treated with antibodies for TH, and sections from two animals were treated with antibodies for CGRP. Of the 130 DRG neurons positive for ChR2-YFP (YFP+) and 156 positive for TH (TH+), only 13 (10%) were positive for both proteins (Figure 1a). The size of YFP+ neurons was significantly different compared to the TH+ neurons ( $t(155)=6.00$ ,  $p<0.001$ ), though there was overlap in the distribution (Figure 1b). Consistent with Li *et al.* (2011) and Brumovsky *et al.* (2012), TH+ neurons were small in diameter, with a peak around  $300 \mu\text{m}^2$ . The YFP+ neurons varied more in size, showing a second peak.

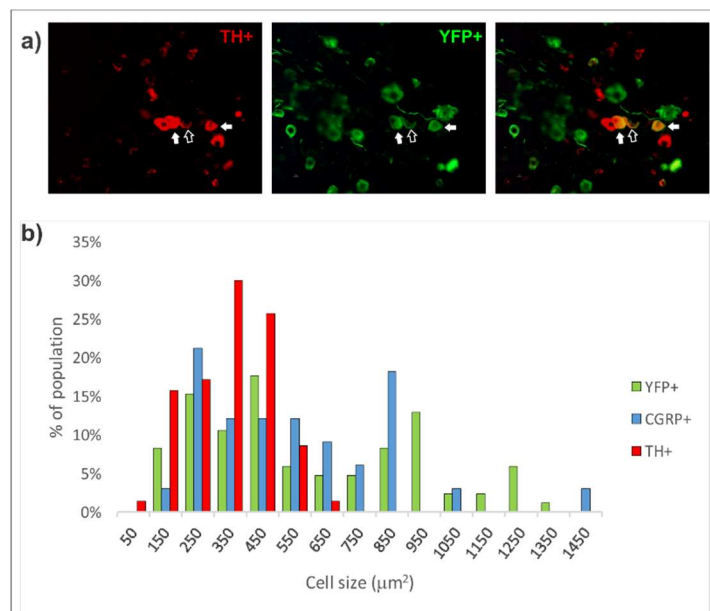


**Figure 1 - Dorsal root ganglia neurons from TH::ChR2-YFP mice.**

Thoracic dorsal root ganglia from adult TH::ChR2-YFP mice were labeled with antibodies of TH, YFP, and/or CGRP. (a) Some cell bodies were labeled strongly by both TH and YFP antibodies (white arrows) and some more weakly (outlined arrows). Many neurons were exclusively either TH+ or YFP+. (b) Size distribution of CGRP+, TH+, and YFP+ neurons in the dorsal root ganglia (34 CGRP+ neurons, 71 TH+ neurons, and 86 YFP+ neurons measured).

Additionally, 1 out of the 58 (1.7%,  $n = 2$ ) YFP+ neurons treated with CGRP antibodies was positive for both proteins, but this is less than expected given reports that 64.5% and 57% of thoracolumbar colorectal and urinary bladder visceral DRG afferents, respectively, co-express TH and CGRP (Brumovsky *et al.*, 2012).

Results were similar in the dorsal cutaneous nerve (DCN). Though there was some overlap in axons expressing TH and ChR2-YFP, other axons were either exclusively TH+ or YFP+ (Figure 2). Some TH+ neurons in the DCN show punctate expression of TH, possibly indicating myelinated TH+ fibers. These myelinated TH+ neurons do not express ChR2-YFP in their axons (Figure 2a),

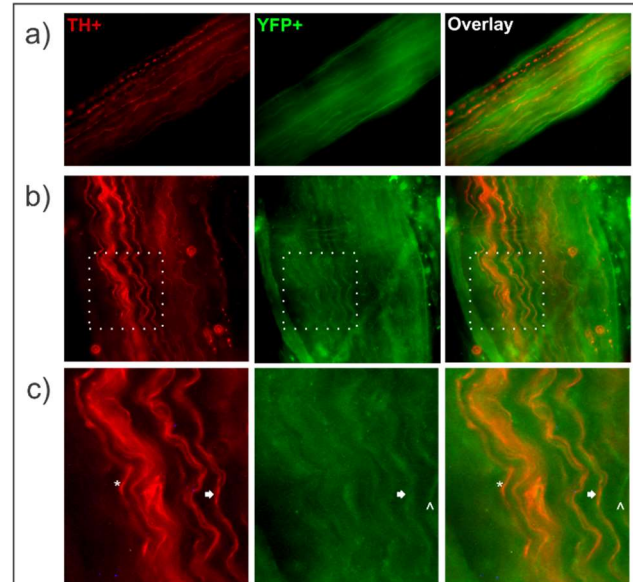


**Figure 2 - TH and ChR2-YFP expression in dorsal cutaneous nerves**  
 (a) Nodal expression of TH in some axons does not overlap with ChR2-YFP expression. (b) Some axons appear to be both TH+ and ChR2-YFP+ while others only express one of the two proteins. (c) Close-up of area in (b), showing axons that are TH+ (\*), ChR2-YFP+ (^), and positive for both proteins (arrow).

though it is unclear if they express the transgene in their terminal end organs.

Beta galactosidase (lacZ) staining of TH::lacZ mouse skin revealed terminal end organs surrounding the hair follicles (Figure 3a and b). A majority of follicles showed beta galactosidase around the base of the follicle (Figure 3b). Whole mount skin sections made it difficult to visualize the specific structure of the end organs through the tissue. On the edges of the skin sections, however, the hair

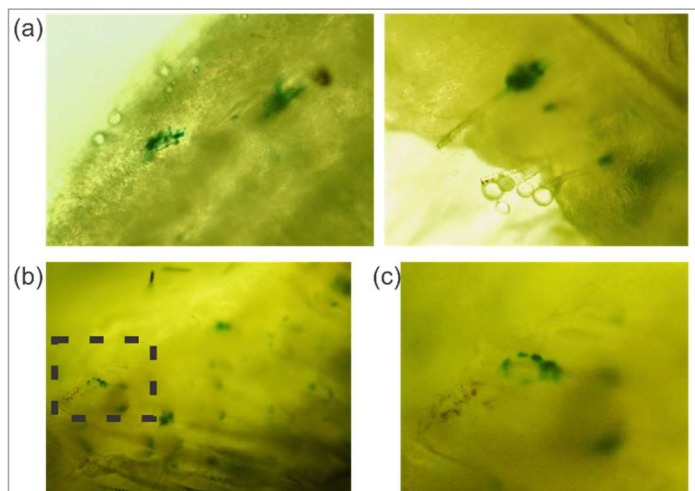


**Figure 3 - TH::lacZ cutaneous end organ  $\beta$ -galactosidase ( $\beta$ -gal) staining**  
 Skin from an adult TH::lacZ mouse showing  $\beta$ -gal staining (a)  $\beta$ -gal staining is evident at the base of hair follicles in the skin. (b)  $\beta$ -gal stained a majority of hair follicles. (c) Close-up of  $\beta$ -gal stained end organ, showing lanceolate endings

follicles were more visible and revealed the characteristic lanceolate endings of follicle-associated LTMRs (Figure 3c).

To visualize the central terminals of ChR2-YFP+ neurons, spinal cord sections were labeled with antibodies against PKC $\gamma$  and CGRP. C-LTMRs are known to project to Rexed lamina IIiv of the mouse spinal cord dorsal horn and overlap with PKC $\gamma$ -

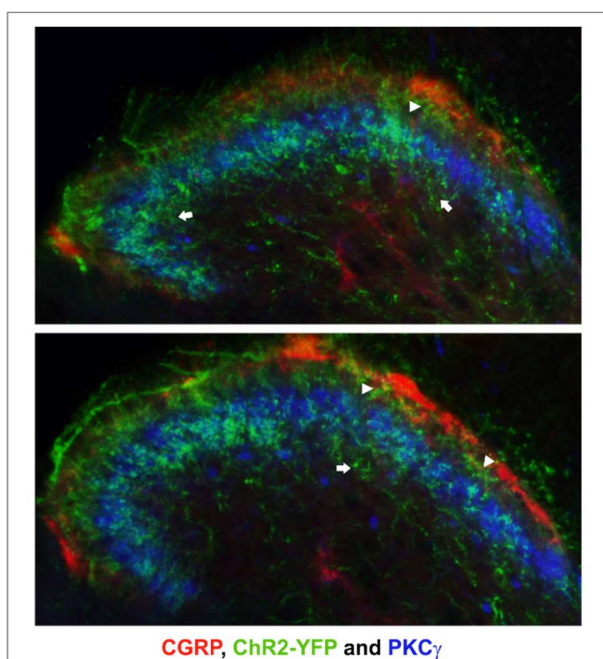


**Figure 4 - Central projections of TH-Cre:ChR2-YFP neurons**  
Immunostaining of CGRP (red), PKC $\gamma$  (blue), and YFP fluorescence (green) in thoracic spinal cord sections shows that the central endings of ChR2-YFP+ neurons overlap extensively with PKC $\gamma$ + interneurons in lamina IIiv of the dorsal horn, though terminals also appear in laminae I, IIo (arrowheads) and III (arrows).

expressing (PKC $\gamma$ +) interneurons (Li *et al.*, 2011), while CGRP-expressing neurons project to laminae I and IIo (Molliver *et al.*, 1995; Tie-Jun, Xu, and Hökfelt, 2001).

A majority of ChR2-YFP+ central axon terminals overlapped with the PKC $\gamma$ + interneurons in lamina III (Figure 4). A small subset of ChR2-YFP+ terminals appeared in more superficial laminae (Figure 4, arrowheads) and in lamina III of the dorsal horn (Figure 4, arrows), but this

phenomenon has been reported in other studies of TH+ C-LTMRs (Bromovsky *et al.*, 2006; Li *et al.*, 2011). This pattern appeared bilaterally in mice from all surgical treatments and at all thoracic spinal levels sampled (T8-T11).

In conclusion, expression is consistent with a non-specific labeling of afferent fiber populations due to early expression of TH in many primary afferents (Ichikawa *et al.*, 2005). That only a small minority of afferents was labeled is consistent with the initial

report of this line leading to sparse labeling of TH expressing neurons (Savitt *et al.*, 2005). Fortuitously, it appears that labeled afferents clearly included prominent distributions in the periphery and centrally that would be expected of C-LTMRs. Also fortuitous is the observation that few small diameter TH::ChR2-YFP neurons were labeled with CGRP – a marker associated with C nociceptors – compared to reports of embryonic TH/CGRP coexpression (Ichikawa *et al.*, 2005) and expression in TH+ visceral afferents (Brumovsky *et al.*, 2012).

### **Electrophysiology:**

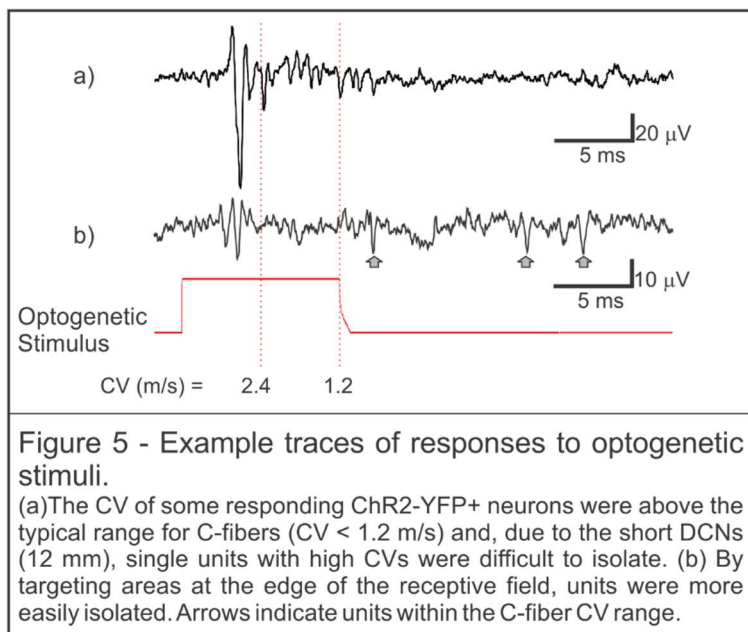
Optogenetic excitation of the dorsal thoracic skin elicited responses from DCN neurons with conduction velocities above and below the C-fiber range, and excitation in the center of the receptive field resulted in compound or overlapping potentials (Figure 5a). By targeting areas of the receptive field with less optogenetic response activity, we were able to identify individual unit responses more effectively (Figure 5b). Units with a CV < 1.2 m/s were compared to those with CV > 1.2 m/s on four measures of spike shape: half-width, peak amplitude, rise slope from 10% to 90% of amplitude, and decay slope from 90% to 10% of amplitude.

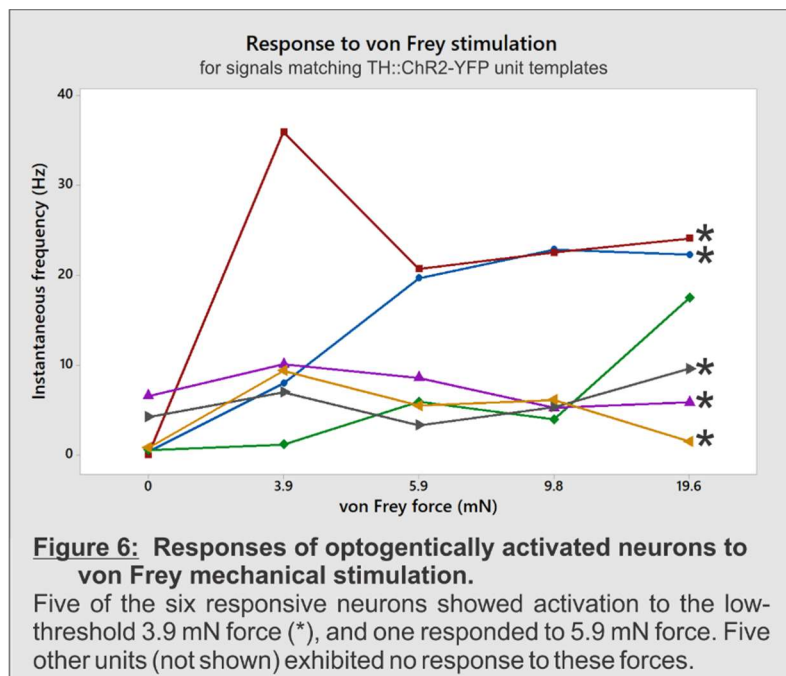
In the 10 TH::ChR2-YFP animals used for optogenetic unit characterization, 44 individual units from 7 different animals were identified and characterized. Responses that fell below the conduction velocity of C-fibers (CV < 1.2 m/s; n=32) were separated from those above this threshold (CV > 1.2 m/s; n=12). Between these two groups, differences in four measures of spike shape were compared: half-width, peak amplitude, rise slope from 10% to 90% of amplitude, and decay slope from 90% to 10%

of amplitude. These groups showed substantial overlap in half-width, peak amplitude, rise slope, and decay slope, and we found no significant difference between the group means of these parameters (Table 2).

Of the individual units recruited by optogenetic stimuli,

eleven were tested for their responses to increasing mechanical stimulation by applying calibrated von Frey filaments to the same area of skin that received the optogenetic stimuli. Optogenetic recordings were used to create spike templates, and the templates were used to search DCN recordings for responses to graded von Frey hairs. Five of the 11 neurons tested did not respond to forces used, and seven showed robust responses to at least one of the von Frey forces, defined by a mean instantaneous frequency (IF) greater than 10 Hz. However, when outliers exceeding 3 standard deviations from the mean IF were removed, only six met this threshold of 10 Hz. Of those six, five units showed increased activity in response to the 3.9 mN stimulus, indicating a threshold  $\leq 3.9$  mN, and the sixth responded to 5.9 mN of force (Figure 6). Three units showed the highest mean instantaneous frequencies (IF) to the low-threshold 3.9 mN von Frey stimuli.



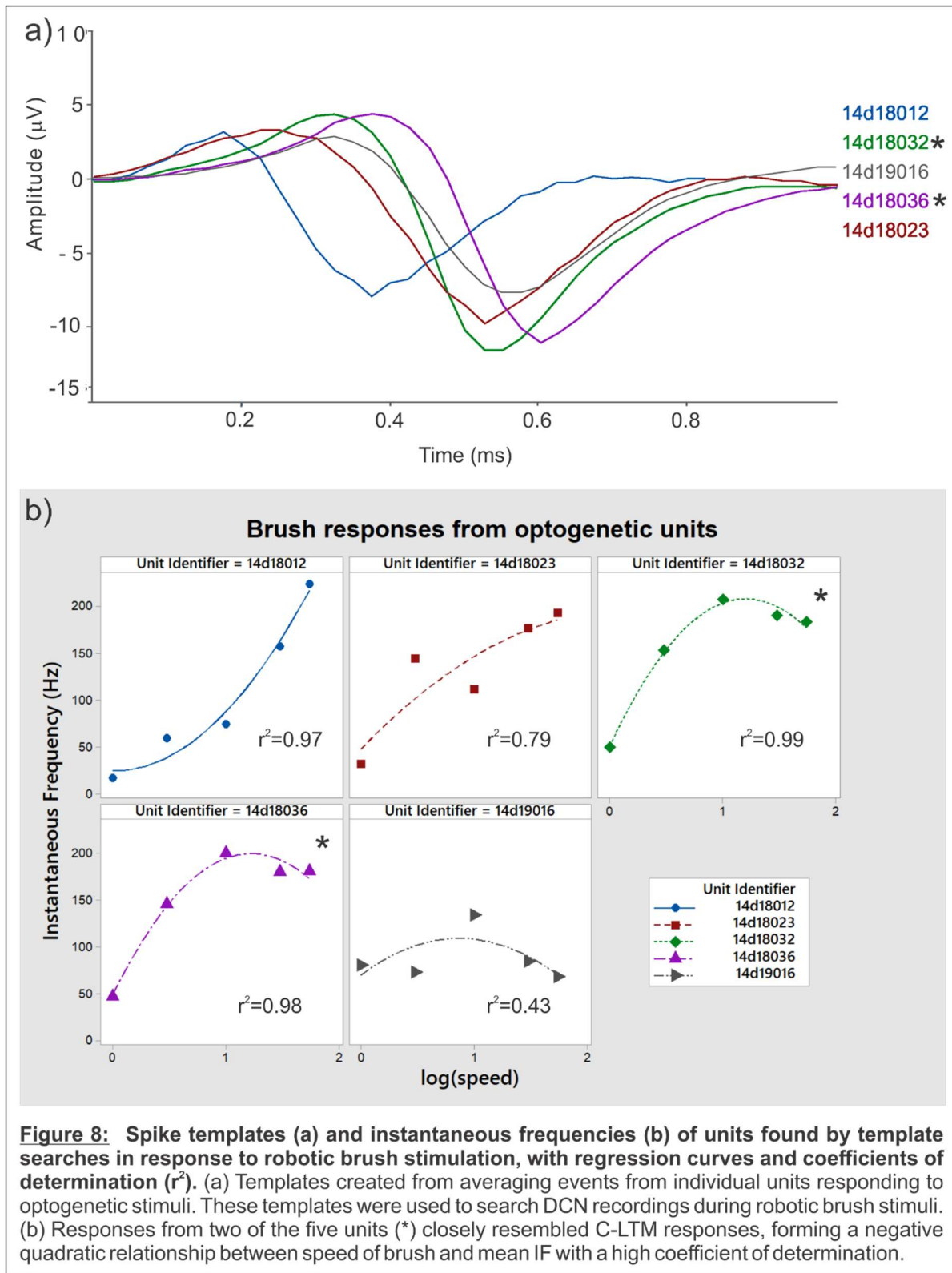


Optogenetic recordings of five other individual units were used to create spike templates to search DCN recordings for responses to robotic brush stimuli (Figure 7a). Mean instantaneous frequency data was averaged for responses at each speed of brush stimuli (1, 2, 10, 30, and 55 cm/s) within

the period of brush contact with the skin. Of the five units recorded, three neurons showed the highest instantaneous frequencies at intermediate brush speeds, and these responses formed negative quadratic curves of best fit (Figure 7b). Only two of the three, however, closely matched the curve of best fit. The other two of these five units increased their response frequencies as speeds increased. Additionally, these two units had the least total number of responses over all speeds (data not shown).

**Table 2 - Mean  $\pm$  SD of action potential measurements for neurons responding to cutaneous optogenetic stimuli.** Parameters of repeated single unit responses ( $289 \pm 110$  events per unit) from DCN recordings were averaged for 44 neurons in 7 animals. Unit responses were classified by CV as either within c fiber range ( $CV < 1.2$  m/s) or above it ( $CV > 1.2$  m/s). A majority of spikes identifiable as individual units were found to be in the c fiber range. No difference in means between the two groups were found to be statistically significant.

	All units (n = 44)	CV < 1.2 m/s (n = 32)	CV > 1.2 m/s (n = 12)
Conduction Velocity (m/s)	1.10 $\pm$ 0.838	0.666 $\pm$ 0.244	2.27 $\pm$ 0.725
Half-width (ms)	0.268 $\pm$ 0.068	0.271 $\pm$ 0.068	0.259 $\pm$ 0.068
Peak Amp ( $\mu$ V)	19.0 $\pm$ 11.0	19.1 $\pm$ 10.6	19.0 $\pm$ 12.3
Decay Slope ( $\mu$ V/ms)	88.2 $\pm$ 57.7	91.1 $\pm$ 57.3	80.6 $\pm$ 60.6
Rise Slope ( $\mu$ V/ms)	105.0 $\pm$ 79.4	105.4 $\pm$ 86.9	104.1 $\pm$ 57.9



### **Action potential differences between ipsilateral and contralateral ChR2-YFP+ units**

To better understand changes in peripheral sensory neurons after SCI, I compared action potential measurements of individual units recorded from DCNs contralateral and ipsilateral to hemisection SCI in response to optogenetic stimulation (19, from  $n = 5$  animals; and 16, from  $n = 4$  animals, respectively). Due to the small sample size of units recorded from sham (5, from  $n = 1$  animal) and uninjured subjects (4, from  $n = 1$  animal), these data were not included in statistical analyses. For each measurement, the absolute value of the mean measurement from repeated recordings of individual units was calculated ( $\mu = 311$ ,  $\sigma = 109$  spike recordings measured and averaged per unit). SCI was confirmed in each animal by the ablation of the PKC $\gamma$  expression in one or both of the dorsal cervicospinal tracts (Mori *et al.*, 1990; Hill, Beattie, and Bresnahan, 2001), but the specific level of injury was confirmed in only two of the five SCI animals.

I initially analyzed all units that were characterized for responding to optogenetic stimuli, both within and above CV range for C-fibers, to identify changes in spike shape. The mean rise slope of units ipsilateral to injury was significantly higher than that of units contralateral to injury ( $\bar{x}_{\text{ipsi}} = 153.9 \mu\text{V/ms}$  and  $\bar{x}_{\text{cont}} = 65.2 \mu\text{V/ms}$ , respectively; Welch's t-test,  $t(16.6) = 3.55$ ,  $p = 0.0025$ ,  $\alpha = 0.01$ , 95% CI [35.88, 141.47]). Units recorded from DCNs ipsilateral to injury trended toward faster conduction velocities, though this trend did not reach significance after an  $\alpha$  adjustment using the Holm-Bonferroni method for multiple comparisons ( $\bar{x}_{\text{ipsi}} = 1.288 \text{ m/s}$  and  $\bar{x}_{\text{cont}} = 0.755 \text{ m/s}$ , respectively; Welch's t-test,  $t(21.7) = 2.19$ ,  $p = 0.0397$ ,  $\alpha = 0.0125$ , 95% CI [0.027, 1.039]). Mean half-width ( $\bar{x}_{\text{ipsi}} = 0.271 \text{ ms}$  and  $\bar{x}_{\text{cont}} = 0.275 \text{ ms}$ ), peak amplitude ( $\bar{x}_{\text{ipsi}} =$

22.7  $\mu\text{V}$  and  $\bar{x}_{\text{cont}} = 15.2 \mu\text{V}$ ), and decay slope ( $\bar{x}_{\text{ipsi}} = 77.8 \mu\text{V}/\text{ms}$  and  $\bar{x}_{\text{cont}} = 84.7 \mu\text{V}/\text{ms}$ ) were not different between these two groups.

When searching for units in ipsilateral skin, I had trouble locating units within the C-fiber CV range. Because I recorded more units above C-fiber CV range in these situations, I decided to analyze only C-fiber units and divide them by both relationship to injury and by spinal level. In this analysis, a two-way ANOVA did not reveal any significant effect of spinal level or relation to injury on mean CV, decay slope, or half-width. However, level and relation to injury did have an effect on peak amplitude and rise slope. Post-hoc comparison of means with a Holt-Bonferroni correction for multiple comparisons revealed that T9 DCN C-fibers had significantly higher peak amplitudes (Welsh's t-tests; T9<sub>ipsi</sub> vs. T9<sub>cont</sub>:  $t(6.06) = 6.13$ ,  $p = 0.0008$ , 95% CI [12.9, 30.1]; T9<sub>ipsi</sub> vs. T10<sub>ipsi</sub>:  $t(2.29) = 5.89$ ,  $p = 0.02$ , 95% CI [9.3, 44.1]) and rise slopes (Welsh's t-tests; T9<sub>ipsi</sub> vs. T9<sub>cont</sub>:  $t(4.19) = 5.68$ ,  $p = 0.0041$ , 95% CI [104, 297]; T9<sub>ipsi</sub> vs. T10<sub>ipsi</sub>:  $t(3.37) = 7.06$ ,  $p = 0.0039$ , 95% CI [136, 335]) than their T9 contralateral or T10 ipsilateral counterparts (Table 3 and Figure 8).

**Table 3 - Mean  $\pm$  SD of action potential measurements for TH::ChR2-YFP C-fiber neurons after T10 hemisection SCI, grouped by level and relationship to injury.** Means compared to T9 ipsilateral, \* $p < .025$ ; \*\* $p < .005$ ; \*\*\* $p < .001$ .

	T9 Ipsilateral (n = 4)	T9 Contralateral (n = 5)	T10 Ipsilateral (n = 2)	T10 Contralateral (n = 10)
CV (m/s)	0.47 $\pm$ 0.089	0.56 $\pm$ 0.204	0.72 $\pm$ 0.265	0.60 $\pm$ 0.171
Half-width (ms)	0.37 $\pm$ 0.078	0.28 $\pm$ 0.059	0.26 $\pm$ 0.081	0.28 $\pm$ 0.042
Peak Amp ( $\mu\text{V}$ )	38.81 $\pm$ 4.802	17.29 $\pm$ 4.310***	12.09 $\pm$ 3.588*	16.26 $\pm$ 3.900
Decay Slope ( $\mu\text{V}/\text{ms}$ )	79.56 $\pm$ 46.082	88.72 $\pm$ 44.570	77.71 $\pm$ 6.509	101.34 $\pm$ 30.636
Rise Slope ( $\mu\text{V}/\text{ms}$ )	287.33 $\pm$ 55.912	86.69 $\pm$ 28.818**	51.92 $\pm$ 8.333**	55.61 $\pm$ 16.124

### Dermatome mapping revealed significant changes in T10 DCN activity.

To assess overall changes in receptive field size and general activity of ChR2-YFP+ neurons in level T9 and T10 DCNs, I systematically exposed each square millimeter of the level T9 and T10 dermatomes to optogenetic stimulation (5 x 10 ms pulses) while recording from T9 and T10 DCNs. To create a measure of neuronal activity for each square millimeter, I took the absolute value of the response and calculated the area under the signal for the time duration corresponding to CV > 1.2 m/s and for CV < 1.2 m/s and averaged this value over all five optogenetic pulses. That mean served as raw measure of overall activity for that one square millimeter of the dermatome. This procedure was repeated for each square millimeter for each DCN on both sides of each SCI animal (n = 5).

For the dermatome average maps (Figure 9), the raw activity data for each DCN dermatome was first scaled to 100 ( $[\text{activity for mm}^2 - \text{minimum of dermatome}] / [\text{maximum} - \text{minimum}]$ ). All scaled activity data for each level, CV range, and relationship to injury combination (i.e. each individual map in Figure 9) was aligned

rostrocaudally so that the maximum scaled activity for the maps was centered on the same row ("0" on the rostrocaudal axis). This scaling process also controlled for baseline

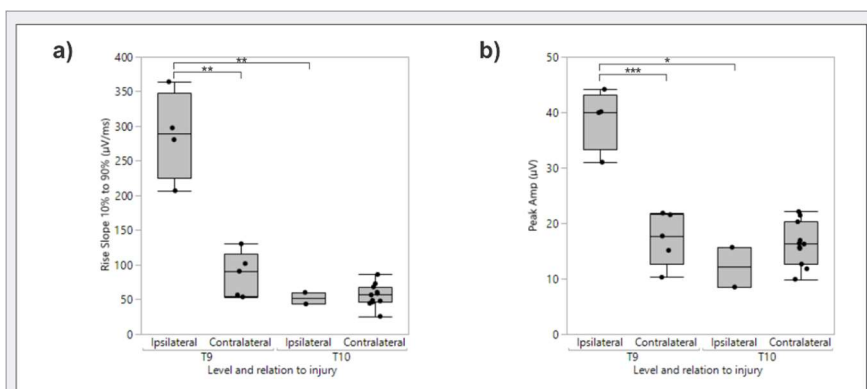


**Figure 8 - Comparison of action potential properties between ChR2-YFP+ C-fiber units by level and relation to SCI.**

Box and whisker plots summarizing the median and interquartile range of individual units recorded from T9 and T10 DCNs contralateral and ipsilateral to level T10 hemisection SCI in response to optogenetic stimuli. Units were included in analysis if they fell within C-fiber CV range (CV < 1.2 m/s). For each measurement, the absolute value of the mean from repeated recordings ( $\mu = 311$ ,  $\sigma = 109$ ) of individual units was calculated. (a) ChR2-YFP+ C-fibers recorded from T9 DCNs ipsilateral to injury showed a significant increase in mean rise slope compared to their T10 counterparts and to contralateral T9 ChR2-YFP+ C-fibers. (e) Mean peak amplitude was significantly higher in level T9 ChR2-YFP+ C-fibers ipsilateral to injury compared to T10 ipsilateral and T9 contralateral ChR2-YFP+ C-fibers.

\* $p < .025$ ; \*\* $p < .005$ ; \*\*\* $p < .001$

activity, as the area with minimal activity was subtracted from each mm<sup>2</sup>. Scaled activity was then averaged across all individuals. I then calculated the area of the dermatome as the number of cells that exceeded the midpoint of the range of the dermatome average map (i.e. scaled score above 50). This conservative threshold for defining activity was based on the observation that some dermatomes had high scaled values outside of the apparent receptive field.

Based on this processing of the data, T9 ipsilateral DCN ChR2-YFP+ neurons with CV < 1.2 m/s appeared to show a decrease in receptive field area compared to T9 contralateral and T10 DCNs. When the area of each subject's T9 ipsilateral dermatome was compared with that of the T9 contralateral dermatome using a paired t-test, there was no difference in dermatome area ( $t(4) = -0.147$ ;  $p = 0.890$ ). This was also true of the T10 ipsilateral and contralateral dermatomes ( $t(2) = 0.1685$ ;  $p = 0.8817$ ).

To better assess the relative intensity of response between ipsilateral and contralateral ChR2-YFP+ neurons, raw activity data for both ipsilateral and contralateral responses were scaled together to 100 at each level and conduction velocity before aligning and averaging across all individuals (i.e. each pair scaled together). This analysis only included animals in which the same recording electrode was used on the same level DCN from both sides of the skin. Cells above the median were averaged to create a relative intensity mean response, and the lower two quartiles were averaged to create a baseline activity level. This processing of the data, which put ipsilateral and contralateral responses on the same scale, revealed significant effects of SCI on ChR2-YFP+ activity (Figure 10). T10 ChR2-YFP+ DCN neurons ipsilateral to injury showed a marked decrease in activity compared to those contralateral to injury across all CV

groups (Welsh's t-test,  $p < 0.001$  for each). The means of the lower 50<sup>th</sup> percentile (baseline) of scaled responses for  $CV > 1.2$  m/s were also significantly different ( $p = 0.006$ ), though the magnitude of the difference in baseline ( $\Delta\bar{x} = 0.45$ ) is unlikely to account for the difference in response intensity ( $\Delta\bar{x} = 9.9$ ). No such differences were found in the T10 baseline means for responses in the C-fiber range ( $CV < 1.2$  m/s) or for the overall response (All CVs). This shows that even though there was no difference in the baseline activity, the response intensities between T10 ipsilateral and contralateral DCNs were significantly different. A Welsh's t-test of the mean response intensity for T9 DCN revealed no difference between ipsilateral and contralateral T9 DCN dermatomes after SCI.

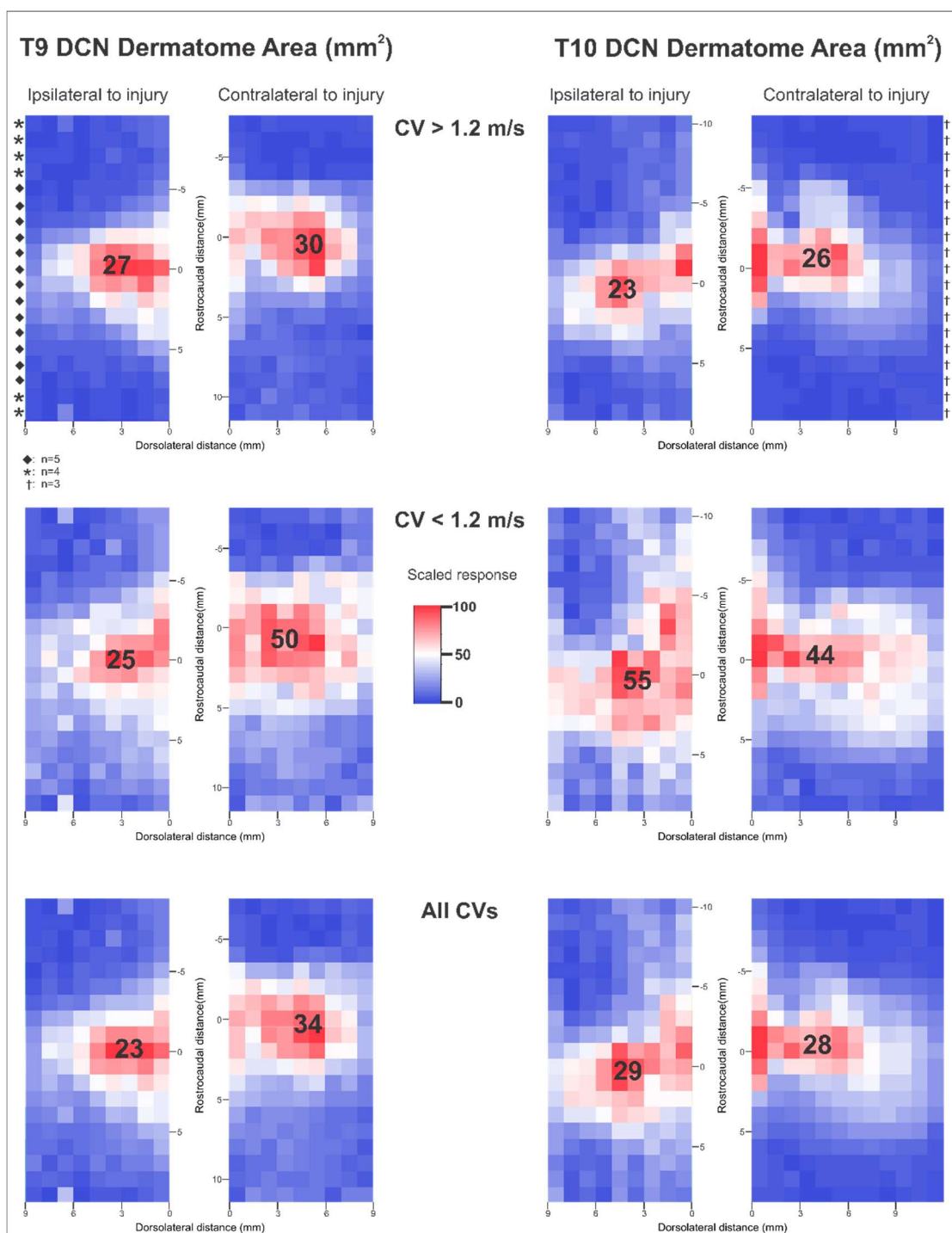
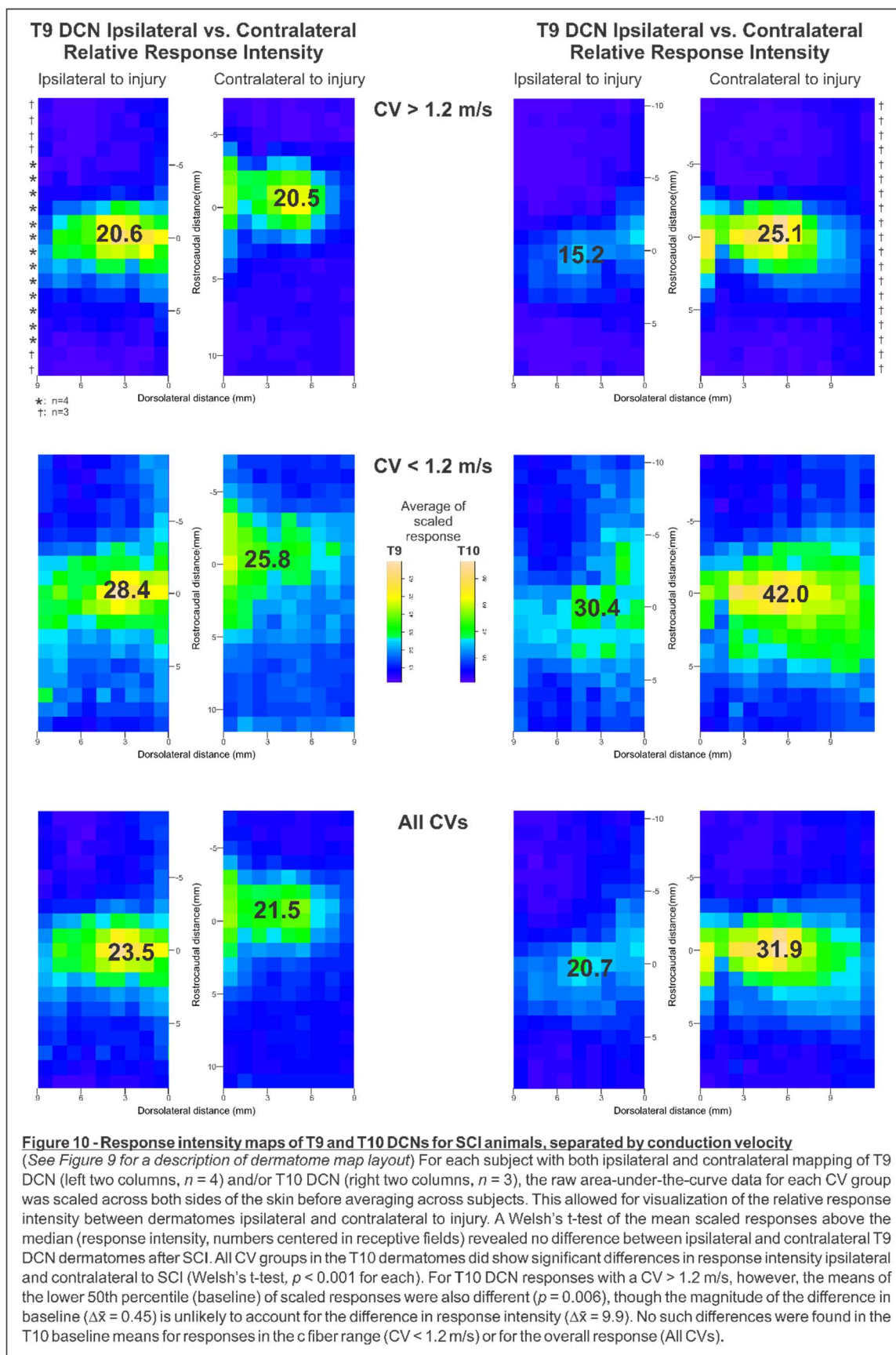


**Figure 9 - Dermatome area of T9 and T10 DCNs for SCI animals, separated by conduction velocity**

Mean area under the curve for recordings of DCN response to optogenetic stimuli was used to map the dermatome of the T9 DCN (left two columns,  $n = 5$ ) and T10 DCN (right two columns,  $n = 3$ ) in mice after recovery from SCI. One square millimeter of the dorsal trunk skin is represented by one pixel in the maps. Responses with a CV > 1.2 m/s (top row) were separated from those with CV < 1.2 m/s (middle row) and then added to create an overall response map (bottom row). The axis between map pairs represents the dorsal midline, with the rostral-to-caudal direction going from top to bottom of the maps. The left and right of each pair represent responses from DCNs ipsilateral and contralateral to SCI, respectively. Numbers within each receptive field depict the number of pixels in the dermatome above the midpoint of the response range for that particular dermatome map. These maps suggest a decrease in dermatome area from T9 DCN sensory neurons, especially from those in the c fiber CV range (CV < 1.2 m/s), and a possible expansion of the dermatome in T10 DCN c fibers.



## Discussion

### **Evaluating the Tg(Th-cre)1Tmd driver for transgene expression in DRG neurons**

My results from immunofluorescence labeling of the DRG show only partial overlap in expression of the ChR2-YFP transgene within TH<sup>+</sup> DRG neurons (Figure 1a). The fact that 13 of 156 TH<sup>+</sup> DRG neurons also expressed ChR2-YFP is consistent with the initial report of this TH-Cre driver line leading to sparse labeling of TH-expressing neurons, though our results show the effectiveness of the driver line in DRG neurons is lower (Savitt *et al.*, 2005). Savitt *et al.* (2005) reported that one-third of TH<sup>+</sup> neurons in the striatum were affected by Cre recombinase expression, and our results are one-fourth of that. It is possible that ChR2-YFP is frequently not expressed in the soma membrane in a sub-population of neurons and may instead be found in the axons and terminal end organs. The fact that an abundance of follicles were stained with beta galactosidase in the TH::lacZ mice and the extensive ChR2-YFP<sup>+</sup> central terminals in lamina II<sub>IV</sub> of the dorsal horn suggest that this may be the case.

In terms of the specificity of the TH-Cre driver strain, I did encounter some overlap between ChR2-YFP and CGRP expression (1/58, n = 2), though this is hardly evidence for ectopic expression of the ChR2-YFP transgene. TH<sup>+</sup> visceral afferents from the colon and the bladder, traveling along the splanchnic nerve, are most abundant at levels T8-T12, and these TH<sup>+</sup> visceral DRG neurons often co-express CGRP (Brumovsky *et al.*, 2012). My results concerning CGRP overlap in DRG (1.7%) were a small fraction of what has been reported for the TH<sup>IRES</sup>-Cre driver strain (84%; Lagerström *et al.*, 2010) and for TH<sup>+</sup> visceral afferents in level T8-T12 DRG (Brumovsky

*et al.*, 2012). Based on the immunohistochemistry counts presented by Brumovsky *et al.* (2012), a result of ~10% overlap would be closer to their results in lower thoracic DRGs.

In the spinal cord, the axon terminals of TH::ChR2-YFP neurons are localized to lamina II<sub>iv</sub> and overlap with PKC $\gamma$  in the dorsal horn (Figure 4), consistent with reports of C-LTMR terminals (Li *et al.*, 2011). The terminals seem to extend further into layer III of the dorsal horn than reports from labelling other proteins found in C-LTMRs such as TAF4A (Delfini *et al.*, 2013) and Na<sub>v</sub>1.8 (Shields *et al.*, 2012), but they seem consistent with previously described TH+ C-LTMR terminals (Li *et al.*, 2011). A similarly encouraging result was found by beta galactosidase staining of the skin. A majority of hair follicles were labeled, and terminal end organs resembled the lanceolate endings of LTMRs (Li *et al.*, 2011). A closer, more detailed, and more systematic analysis using confocal microscopy should be used to confirm that the structure of the terminal end organs in a majority of follicles are consistent with C-LTMRs as opposed to the varicose endings of catecholaminergic efferent neurons innervating piloerector muscles (Schotzinger and Landis, 1990). Finally, the responses to mechanical stimuli based on optogenetic unit template searches provides further supporting evidence that TH::ChR2-YFP neurons include populations of TH+ C-LTMRs.

C-LTMRs have a low threshold of activation (< 5 mN) compared to high-threshold C-fiber mechanoreceptors ( $\geq$  10 mN) (Valbo, Olausson, and Wessberg, 1999). Using templates from optogenetically activated units, I searched recordings of calibrated von Frey stimuli in the same location on the skin. Four of the 11 templates identified units responding to von Frey threshold forces of 3.9 mN. The threshold of a fifth unit fell between 3.9 and 5.9 mN. Because I did not find action potential differences between the

myelinated and unmyelinated ChR2-YFP+ neurons characterized, I cannot rule out that the templates may have identified myelinated LTMRs. However, as a control measure, when I used these five low-threshold templates to search other recordings of von Frey stimuli outside of their receptive fields, this procedure did not reveal such responses. This provides evidence that a subset of the ChR2-YFP+ cutaneous neurons are TH+ C-LTMRs.

Further support for the recruitment of TH+ C-LTMRs can be found in the responses to robotic brush stimuli. CT afferents in humans have been shown to form negative quadratic, or inverted U-shaped, curves in response to increased speed of brush stroke, with a peak between 1-10 cm/s (Löken *et al.*, 2009). I found two of the five recorded units tested for brush speed responded in a similar manner (Figure 7b). Our data in mice indicate that mouse TH+ C-LTMRs reach peak instantaneous frequency at faster speeds, with peak response at 10 cm/s (Figure 7b). This reproduces Andrew's (2010) result of peak responses in wide dynamic range spinoparabrachial neurons responding to brush strokes in which the maximum occurred at a mean brush velocity of 9.2 cm/s. An increased peak velocity for C-LTMRs in mice is not surprising given the speed of mouse allogrooming and self-grooming behavior. The reported response frequencies reported by Andrew (2010), however, were roughly half of those from our TH+ C-LTMRs. Taken together, this study produced convincing evidence that TH::ChR2-YFP animals express the ChR2 transgene in the C-LTMR population.

Although C-LTMRs are purported to be the only cutaneous sensory afferents that express TH in the adult mouse (Li *et al.*, 2011), other cutaneous neurons in our TH::ChR2-YFP mouse model are also likely to express the ChR2-YFP transgene. TH is

expressed by peripheral sympathetic neurons (von Euler, 1971), and Brumovsky, Villar, and Hökfelt (2006) found extensive TH<sup>+</sup> sympathetic innervation of blood vessels and glabrous skin sweat glands in addition to hair follicles. Though the lanceolate end organs of TH<sup>+</sup> C-LTMR are found in hair follicles (Li *et al.*, 2011), so are the catecholaminergic efferent neurons innervating piloerector muscles (Schotzinger and Landis, 1990). Furthermore, the number of ChR2-YFP<sup>+</sup>/TH<sup>-</sup> neurons and the difference in size distribution between TH<sup>+</sup> immunolabeled neurons and ChR2-YFP<sup>+</sup> neurons raise questions regarding specificity and ectopic expression of the ChR2-YFP transgene outside of the adult TH<sup>+</sup> neuronal population. According to electrophysiology results, large amplitude responses at faster CVs suggest that our model expresses ChR2-YFP<sup>+</sup> in some myelinated cutaneous sensory neurons.

These myelinated afferents most likely express the ChR2-YFP transgene due to transient developmental TH expression. TH is expressed transiently during prenatal development in several structures where it is absent in the adult (Jonakait *et al.*, 1984). Since Cre-mediated genomic recombination is not reversible, these structures should continue to express ChR2-YFP throughout the life of the neuron despite ceasing TH expression. When using a dopamine beta hydroxylase-driven Cre strain, the next enzyme in catecholamine production after TH, Matsushita *et al.* (2004) found that both large (soma area 1000-1600  $\mu\text{m}^2$ ) and small (200-600  $\mu\text{m}^2$ ) neurons showed recombination in DRG sections. Though their animals showed fewer smaller than larger DRG neurons, it is likely that the populations are similar to our model. A study involving immunohistochemistry on embryonic DRGs found similar size discrepancies and noted that 15.1% of TH immunoreactive DRGs were also labeled with CGRP antibodies

(Ichikawa *et al.*, 2005). Our Cre driver strain did not show this same level of co-expression with CGRP, fortunately. Franck *et al.* (2011) found that 60 % of DRG neurons expressed TH at 13.5 days after conception, and these TH+ neurons were TrkA+/Ret-, leading them to believe they identified the late TrkA population (Franck, 2013). This population of neurons is not fully understood but likely includes C-fiber nociceptors and A $\delta$ -fibers that express TRPV1 and CGRP (Franck *et al.*, 2011; Franck, 2013). Though not included in my immunohistochemistry results, I also encountered 4 YFP+ neurons co-labeled with TRPV1 antibodies, but very few DRG sections from only one animal were treated with TRPV1 antibodies. These were not systematically photographed or counted and therefore were not included in any analyses. This TH+/TRPV1+ result is consistent with reports of the majority of TH+ visceral afferents co-expressing TRPV1 (Brumovsky *et al.*, 2012), but further analysis of TH/TRPV1 co-expression would be necessary to compare the frequency of these events to those of Brumovsky *et al.* (2012) or to conclude that they represent cutaneous afferents with transient developmental TH expression.

Therefore, this model drives ChR2-YFP expression in more DRG neurons than just adult TH+ C-LTMRs, but whether from TH promoter activity in precursor cell populations or ectopic expression remains unclear. A first step in this process would be to better identify the units recruited during cutaneous optogenetic stimulation. Recording from DRG neurons while mechanically and optogenetically activating individual units would be the most direct way of solving this problem. Activity-dependent CV slowing has been used to identify C-fibers as either nociceptors or C-LTMRs in the rat and human saphenous nerve (Gee *et al.*, 1996), but this technique was recently

unsuccessful and non-specific in mice (Hoffmann *et al.*, 2015). Measures of CV slowing are also ineffective at distinguishing C-LTMRs from unmyelinated sympathetic postganglionics (Hoffman *et al.*, 2015). However, if the goal is to prevent the expression of ChR2-YFP in TH-transient cutaneous afferents altogether, future studies should employ an inducible TH-Cre recombinase driver line (TH-CreER) and induce recombination of the transgene at birth, when TH expression in the DRG is lowest (Franck *et al.*, 2011), or two weeks after birth, when all sensory afferents are committed to their phenotype (Koltzenburg *et al.*, 1997).

### **Effects of SCI on TH::ChR2-YFP cutaneous neurons**

Despite the fact that TH::ChR2-YFP mice express the ChR2-YFP transgene in other cutaneous neurons, I was able to detect changes in axonal spike properties above-level (T9) and decreased activity at-level (T10) after SCI. Conclusions are limited by an insufficient number of sham and uninjured control mice, however, to directly connect these changes to the SCI itself. Despite this limitation, this model has proven the usefulness of using transgenic mice expressing ChR2 in sensory neurons to analyze peripheral changes in response to SCI.

Surprisingly, two of the five axonal spike shape properties evaluated, rise slope and peak amplitude, changed in ipsilateral C-fiber neurons above (T9) but not at the level of SCI (T10). The T10 ipsilateral C-fiber action potential properties were all within the range of contralateral C-fibers. The means of other action potential measurements seemed to differ between contralateral and ipsilateral units (area under the action potential, decay time, rise time, time to antipeak, rise tau, and max rise slope), but these

measurements were not planned comparisons in the experimental design, therefore differences were not statistically tested in order to retain a reasonable alpha significance level for multiple comparisons.

The increase in rise slope and in peak amplitude could be a product of increased insertion of specific voltage-gated sodium channels ( $\text{Na}_v$ ) in the axons of DRG neurons. C-LTMRs express  $\text{Na}_v1.7$  at the highest levels, but they also contain  $\text{Na}_v1.1$ ,  $\text{Na}_v1.2$ ,  $\text{Na}_v1.6$ ,  $\text{Na}_v1.8$ , and  $\text{Na}_v1.9$  (Usoskin *et al.*, 2014). These  $\text{Na}_v$  channels, especially  $\text{Na}_v1.7$ - $1.9$ , have been shown as particularly important in the pathophysiology of different pain syndromes, including neuropathic pain (for review, see Dib-Hajj, Black, and Waxman, 2009). Nociceptive neurons, for example, have longer rising phases and action potential durations due to greater expression of tetrodotoxin-resistant  $\text{Na}_v1.7$ ,  $\text{Na}_v1.8$ , and/or  $\text{Na}_v1.9$  (see Pitcher, Le Pichon, and Chesler, 2016). The sensory terminals and unmyelinated axons of C-fibers have been shown to express receptors for allosteric mediators, including acetylcholine, serotonin, and ATP (Lang *et al.*, 2002, 2003, 2006; Lang and Grafe, 2007). These receptors may allow the C-fibers to adjust their physiology in response to the biochemical environment around them. By altering the ratio of expression of  $\text{Na}_v$  subtypes, as well as alpha and beta subunits, peripheral C-fibers can change action potential properties in response to signals in the periphery.

The most striking differences between contralateral and ipsilateral TH::ChR2-YFP neuron activity after SCI is made apparent by the heat maps from optogenetic dermatome mapping. The dermatome average map (Figure 9), however, does not definitively show true changes in dermatome areas. Although the T9 ipsilateral C-fiber dermatome appears to be smaller than others, it is likely that the increase in amplitude

of the T9 ipsilateral ChR2-YFP+ neurons increased the midpoint of the response range to the point that fewer samples rated above the midpoint, therefore decreasing the area of the dermatome. This interpretation is supported by the activity maps, in which ipsilateral and contralateral responses in each animal were normalized together before averaging across subjects. In these comparisons, the area of the dermatome indicated by the ipsilateral activity map appears to equal or exceed the dermatome area of contralateral T9 C-fibers. Conversely, the 25% increase in area of the T10 ipsilateral C-fiber dermatome is likely an artifact of the decreased overall activity of those ChR2-YFP+ neurons. In fact, locating single units in the T10 ipsilateral skin that fell within C-fiber CV range proved difficult. Only two were able to be characterized across the three SCI animal subjects. Furthermore, the narrow range of activity in the T10 ipsilateral skin led to the dermatome maps of individual subjects showing high scaled activity scores outside of the T10 dermatome. These cases led me to conservatively define the threshold of inclusion in the dermatome as a scaled score of 50, decreasing the accuracy of the dermatome area measurements.

An alternative explanation for the apparent SCI-induced differences in dermatome might be that injury to central T9 C-LTMR terminals in the dorsal horn, or along the dorsal roots, resulted in denervation and shrinking of the ipsilateral T9 dermatome and sprouting from T10 dermatome afferents into the T9 territory. While this cannot be ruled out, results of previous studies make this unlikely. Katz and Black (1986) found that peripheral axotomy reversibly decreased TH in the glossopharyngeal petrosal ganglion, but dorsal rhizotomy, a central nerve injury model that cuts dorsal roots of sensory afferents, failed to alter TH expression in DRG neurons. In peripheral

nerve injury, the expression of TH is typically downregulated, but central injury does not cause changes in TH expression (see Brumovsky, 2016). Conflicting with these results, however, Seal *et al.* (2009) saw a disappearance of ipsilateral VGLUT3 immunoreactivity, another C-LTMR marker, in the dorsal horn after dorsal rhizotomy. This could be a result of the specific disappearance of VGLUT3 interneurons, however, that were later identified in the dorsal horn (Lou *et al.*, 2013). Furthermore, when Jackson and Diamond (1984) cut the DCNs adjacent to T13 DCN, LTMRs did not sprout into adjacent dermatomes when the T13 DCN was left intact, and they sprouted mostly rostrocaudally only when the lateral T13 DCN branch was also cut. In another study, A $\beta$ -LTMRs sprouted into adjacent dermatomes, but only during a critical period at age 15-20 days (Jackson and Diamond, 1981). High threshold mechanoreceptors did not show this critical period for sprouting from the saphenous nerve of the paw, but researchers were unable to identify LTMR sprouting (Devor *et al.*, 1979).

The largest effect of SCI in this study was the decrease in peripheral neuron activity at the level of injury, the T10 DCN dermatome (Figure 10). This overall decrease in activity was confirmed by the difficulty I experienced in finding individual units to characterize in T10 ipsilateral dermatomes.

It would be reasonable to conclude that this activity decrease from at-level ipsilateral TH::ChR2-YFP neurons – if they are primarily TH+ C-LTMRs – could contribute to the symptoms of at-level allodynia. C-LTMRs release both glutamate and the analgesic TFAFA4 in the dorsal horn, and TFAFA4 knock-outs experienced enhanced allodynia that was abolished with injection of exogenous TFAFA4 into the dorsal horn (Delfini *et al.*, 2013). This conclusion, however, would ignore the extensive circuitry of

interneurons in the dorsal horn, of which the C-LTMR input is only one factor. To better understand how this decrease in activity affects allodynic pain perception, a next step would be to compare pain measures in response to brush stroke (all LTMRs activated) to those in response to optogenetic stimuli (C-LTMR activation only).

Cav3.2, a T-type calcium channel expressed by C-LTMRs and A $\delta$ -LTMRs, may play a role in the observed decrease in activity of C-LTMRs at the level of injury. Cav3.2 is expressed in the terminals and axons of C-LTMRs, lowering activation threshold, increasing firing frequency, and increasing action potential fidelity (François *et al.*, 2015). A downregulation of these channels in response to extracellular signals or blocking of the T-type Ca<sup>2+</sup> current would effectively decrease the activity of C-LTMRs. Additionally, Cav3.2 has been shown to respond to modulation by a multitude of endogenous ligands (see Zhang *et al.*, 2013). However, counter to the hypothesis that a decrease of C-LTMR activity would lead to a decrease in analgesic TFAFA4 release in the dorsal horn, conditional knockout of Cav3.2 in C-LTMRs decreased their activity and simultaneously decreased allodynia (François *et al.*, 2015). This could also be a result of an unnatural unbalancing of the glutamate and TFAFA4 release due to the Cav3.2 knockout. Though the identity of the light touch primary sensory population that conveys mechanical allodynia is still unknown, the current preponderance of evidence points to A $\beta$ -LTMRs as the sources of the re-encoded innocuous input (see Arcourt and Lechner, 2015; Koch, Acton, and Goulding, 2018). The evidence presented here of decreased C-LTMR activity at-level supports the idea that C-LTMR input to the dorsal horn interneurons serve as a gate to prevent A $\beta$ -LTMR signals from reaching the lamina I

projection neurons that encode and transmit pain signals to the cortex (see Koch, Acton, and Goulden, 2018).

### **Conclusion**

Allodynia is a common at-level pain syndrome after SCI that greatly decreases the patient's quality of life and may contribute to the development of affective disorders in SCI patients. Recent research has shown that the C-LTMRs play a role in mediating allodynia, but the specifics of that role and the application to SCI-induced pain remain unclear. In this study, I used TH::ChR2-YFP mice to assess changes in TH+ C-LTMRs that might alter the modulation of sensory information in the dorsal horn and contribute to the creation of allodynia.

In the first set of experiments, I confirmed the expression of the ChR2-YFP transgene in TH+ C-LTMRs using histochemical, immunohistochemical, optogenetic, and electrophysiological methods. ChR2-YFP was found in DRG cells overlapping with TH+ neurons, though a majority of ChR2-YFP+ neurons were TH-. In the dorsal horn of the spinal cord, ChR2-YFP was prominently expressed in Rexed lamina IIiv, overlapping extensively with PKC $\gamma$ , similar to the previously described axon terminal locations of C-LTMRs. Expression in the skin showed that recombination was associated with the bases of hair follicles and appeared to form the characteristic lanceolate endings of the cutaneous C-LTMRs. Recordings from DCNs confirmed that the axonal spike shapes of some TH::ChR2-YFP cutaneous neurons were also present in von Frey threshold and robotic brush stimuli recordings, and a subset of these followed the response patterns of C-LTMRs. Though other myelinated and possibly unmyelinated axons responded to optogenetic activation of the ChR2-YFP transgene,

possibly due to transient developmental expression, the presence and functionality of ChR2 in TH+ C-LTMRs was confirmed.

I then sought to characterize how SCI affects C-LTMR activity and physiology several weeks following transverse thoracic ipsilateral hemisection of the spinal cord compared to its opposite contralateral unlesioned side. I examined activity at- and above the segmental lesion level. Transverse hemisection SCI caused a change in axonal membrane physiology of TH::ChR2-YFP C-fibers one spinal segment above the level of injury. Specifically, action potential rise slope and peak amplitude were increased in the DCN TH::ChR2-YFP C-fibers. This change in axon physiology is likely a product of alterations in the expression of voltage-gated ion channels in the C-fibers, possibly mediated by receptors responding to signals in the periphery. Compared to the uninjured side, hemisection SCI also caused a significant decrease in TH::ChR2-YFP sensory neuron activity at the level of injury, including the TH+ C-LTMRs. This alteration in physiology above-level and activity at-level would alter the input to the dorsal horn interneurons responsible for processing innocuous touch, including the PKC $\gamma$  neurons in lamina II<sub>IV</sub>, that could subsequently impact ascending nociceptive pathways. If so, targeting the ion channels involved in altering physiology or increasing activity of certain populations at the level of injury could serve as effective targets to control symptoms of at-level allodynia.

This study is the first to identify changes in C-LTMR activity and physiology in response to SCI. Though the TH::ChR2-YFP mouse model does not exclusively activate TH+ C-LTMRs – possibly due to the recombination of unidentified transiently-expressing TH DRG neurons – the model does allow for precise dermatome mapping to

evaluate SCI-induced changes in TH::ChR2-YFP neurons. Further studies using single-unit recording techniques in the DRG would help identify the transiently-expressing TH neurons and expand the current knowledge of sensory neuron diversification in development. The results of this study also implicate the change in peripheral activity and physiology in the development of SCI-induced at-level allodynia.

## References

- Abraira VE et al. (2017) The Cellular and Synaptic Architecture of the Mechanosensory Dorsal Horn. *Cell* 168:295–310.
- Abraira VE, Ginty DD (2013) The sensory neurons of touch. *Neuron* 79:618–639.
- Andrew D (2010) Quantitative characterization of low-threshold mechanoreceptor inputs to lamina I spinoparabrachial neurons in the rat. *The Journal of Physiology* 588:117–124.
- Arcourt A, Lechner SG (2015) Peripheral and spinal circuits involved in mechanical allodynia. *Pain* 156:220–221.
- Arenkiel BR, Peca J, Davison IG, Feliciano C, Deisseroth K, Augustine GJ, Ehlers MD, Feng G (2007) In vivo light-induced activation of neural circuitry in transgenic mice expressing channelrhodopsin-2. *Neuron* 54:205–218.
- Basso DM, Fisher LC, Anderson AJ, Jakeman LB, Mctigue DM, Popovich PG (2006) Basso Mouse Scale for Locomotion Detects Differences in Recovery after Spinal Cord Injury in Five Common Mouse Strains. *Journal of Neurotrauma* 23:635–659.
- Bessou P, Burgess P, Perl E, Taylor C (1971) Dynamic properties of mechanoreceptors with unmyelinated (C) fibers. *Journal of Neurophysiology* 34:116–131.
- Björnsdotter M, Morrison I, Olausson H (2010) Feeling good: on the role of C fiber mediated touch in interoception. *Experimental brain research Experimentelle Hirnforschung Expérimentation cérébrale* 207:149–155.
- Blomqvist A, Zhang ET, Craig a D (2000) Cytoarchitectonic and immunohistochemical characterization of a specific pain and temperature relay, the posterior portion of the ventral medial nucleus, in the human thalamus. *Brain: a journal of neurology* 123:601–619.
- Bretag AH (1969) Synthetic interstitial fluid for isolated mammalian tissue. *Life Sciences* 8:319–329.
- Brumovsky PR, La JH, McCarthy CJ, Hökfelt T, Gebhart GF (2012) Dorsal root ganglion neurons innervating pelvic organs in the mouse express tyrosine hydroxylase. *Neuroscience* 223:77–91.
- Brumovsky PR (2016) Dorsal root ganglion neurons and tyrosine hydroxylase - An intriguing association with implications for sensation and pain. *Pain* 157:314–320.
- Brumovsky P, Villar MJ, Hökfelt T (2006) Tyrosine hydroxylase is expressed in a subpopulation of small dorsal root ganglion neurons in the adult mouse. *Experimental Neurology* 200:153–165.
- Cairns DM, Adkins RH, Scott MD (1996) Pain and depression in acute traumatic spinal cord injury: origins of chronic problematic pain? *Archives of Physical Medicine and Rehabilitation* 77:329–335.

- Calmels P, Mick G, Perrouin-Verbe B, Ventura M (2009) Neuropathic pain in spinal cord injury: Identification, classification, evaluation. *Annals of Physical and Rehabilitation Medicine* 52:83–102.
- Clements JD, Bekkers JM, Curtin J (1997) Detection of Spontaneous Synaptic Events with an Optimally Scaled Template. *Biophysical Journal* 73:220–229.
- Christensen MD, Hulsebosch CE (1997) Chronic Central Pain after Spinal Cord Injury. *Journal of Neurotrauma* 14:8, 517-537.
- Craig A (2008) Interoception and emotion: a neuroanatomical perspective. In: *Handbook of emotions*, 3rd ed. (Lewis M, Haviland-Jones JM, Barrett LF, eds). The Guilford Press.
- David BT, Sampath S, Dong W, Heiman A, Rella CE, Elkabes S, Heary RF (2014) A Toll-Like Receptor 9 Antagonist Improves Bladder Function and White Matter Sparing in Spinal Cord Injury. *Journal of Neurotrauma* 31:1800–1806.
- Delfini M-C, Mantilleri A, Gaillard S, Hao J, Reynders A, Malapert P, Alonso S, François A, Barrere C, Seal R, Landry M, Eschallier A, Alloui A, Bourinet E, Delmas P, Le Feuvre Y, Moqrich A (2013) TFAFA4, a Chemokine-like Protein, Modulates Injury-Induced Mechanical and Chemical Pain Hypersensitivity in Mice. *Cell Reports* 5:378–388.
- Devor M, Schonfeld D, Seltzer Z, Wall PD (1979) Two modes of cutaneous reinnervation following peripheral nerve injury. *Journal of Comparative Neurology* 185:211–220.
- Dib-Hajj SD, Black JA, Waxman SG (2009) Voltage-gated sodium channels: Therapeutic targets for pain. *Pain Medicine* 10:1260–1269.
- Franck MCM, Stenqvist A, Li L, Hao J, Usoskin D, Xu X, Wiesenfeld-Hallin Z, Ernfors P (2011) Essential role of Ret for defining non-peptidergic nociceptor phenotypes and functions in the adult mouse. *European Journal of Neuroscience* 33:1385–1400.
- Franck MCM. (2013). Genetic control of sensory neuron diversification. Ph.D. Karolinska Institutet, Stockholm, Sweden. Available at: <https://publications.ki.se/xmlui/handle/10616/41386> [Accessed July 8, 2014].
- François A, Schüetter N, Laffray S, Sanguesa J, Pizzoccaro A, Dubel S, Mantilleri A, Nargeot J, Noël J, Wood JN, Moqrich A, Pongs O, Bourinet E (2015) The Low-Threshold Calcium Channel Cav3.2 Determines Low-Threshold Mechanoreceptor Function. *Cell Reports* 10:370–382.
- Gee M, Lynn B, Cotsell B (1996) Activity-dependent slowing of conduction velocity provides a method for identifying different functional classes of C-fibre in the rat saphenous nerve. *Neuroscience* 73:667–675.
- Gordon I, Voos AC, Bennett RH, Bolling DZ, Pelphrey K A, Kaiser MD (2013) Brain mechanisms for processing affective touch. *Human Brain Mapping* 34:914–922.

- Hill CE, Beattie MS, Bresnahan JC (2001) Degeneration and sprouting of identified descending supraspinal axons after contusive spinal cord injury in the rat. *Experimental Neurology* 171:153–169.
- Hoffmann T, De Col R, Messlinger K, Reeh PW, Weidner C (2015) Mice and rats differ with respect to activity-dependent slowing of conduction velocity in the saphenous peripheral nerve. *Neuroscience Letters* 592:12–16.
- Ichikawa H, Mo Z, Xiang M, Sugimoto T (2005) Brn-3a deficiency increases tyrosine hydroxylase-immunoreactive neurons in the dorsal root ganglion. *Brain Research* 1036:192–195.
- Iggo A (1960) CUTANEOUS MECHANORECEPTORS WITH AFFERENT C FIBRES. *The Journal of Physiology* 152:337–353.
- Jackson PC, Diamond J (1981) Regenerating axons reclaim sensory targets from collateral nerve sprouts. *Science (New York, NY)* 214:926–928.
- Jackson PC, Diamond J (1984) Temporal and spatial constraints on the collateral sprouting of low-threshold mechanosensory nerves in the skin of rats. *The Journal of Comparative Neurology* 226:336–345.
- Jakeman LB, Chen Y, Lucin KM, McTigue DM (2006) Mice lacking L1 cell adhesion molecule have deficits in locomotion and exhibit enhanced corticospinal tract sprouting following mild contusion injury to the spinal cord. *The European Journal of Neuroscience* 23:1997–2011.
- Jonakait GM, Markey KA, Goldstein M, Black IB (1984) Transient expression of selected catecholaminergic traits in cranial sensory and dorsal root ganglia of the embryonic rat. *Developmental Biology* 101:51–60.
- Jones RCW III, Xu L, Gebhart GF (2005) The mechanosensitivity of mouse colon afferent fibers and their sensitization by inflammatory mediators require transient receptor potential vanilloid 1 and acid-sensing ion channel 3. *The Journal of Neuroscience* 25:10981–10989.
- Katz DM, Black IB (1986) Expression and regulation of catecholaminergic traits in primary sensory neurons: relationship to target innervation in vivo. *The Journal of Neuroscience* 6:983–989.
- Keller AF, Beggs S, Salter MW, De Koninck Y (2007) Transformation of the output of spinal lamina I neurons after nerve injury and microglia stimulation underlying neuropathic pain. *Molecular Pain* 3:1–11.
- Koch SC, Acton D, Goulding M (2018) Spinal Circuits for Touch, Pain, and Itch. *Annual Review of Physiology* 80:189–217.
- Koltzenburg M, Stucky CL, Lewin GR (1997) Receptive properties of mouse sensory neurons innervating hairy skin. *Journal of Neurophysiology* 78:1841–1850.

- Lagerström MC, Rogoz K, Abrahamsen B, Persson E, Reinius B, Nordenankar K, Ölund C, Smith C, Mendez JA, Chen ZF, Wood JN, Wallén-Mackenzie Å, Kullander K (2010) VGLUT2-Dependent Sensory Neurons in the TRPV1 Population Regulate Pain and Itch. *Neuron* 68:529–542.
- Lang PM, Burgstahler R, Sippel W, Irnich D, Schlotter-Weigel B, Grafe P (2003) Characterization of neuronal nicotinic acetylcholine receptors in the membrane of unmyelinated human C-fiber axons by in vitro studies. *Journal of Neurophysiology* 90:3295–3303.
- Lang PM, Grafe P (2007) Chemosensitivity of unmyelinated axons in isolated human gastric vagus nerve. *Autonomic Neuroscience: Basic & Clinical* 136:100–104.
- Lang PM, Moalem-Taylor G, Tracey DJ, Bostock H, Grafe P (2006) Activity-dependent modulation of axonal excitability in unmyelinated peripheral rat nerve fibers by the 5-HT(3) serotonin receptor. *Journal of Neurophysiology* 96:2963–2971.
- Lang PM, Tracey DJ, Irnich D, Sippel W, Grafe P (2002) Activation of adenosine and P2Y receptors by ATP in human peripheral nerve. *Naunyn-Schmiedeberg's Archives of Pharmacology* 366:449–457.
- Levitt M, Spector S, Sjoerdsma A, Udenfriend S (1965) Elucidation of the rate-limiting step in norepinephrine biosynthesis in the perfused guinea-pig heart. *Journal of Pharmacology and Experimental Therapeutics* 148,1:1-8.
- Li L, Rutlin M, Abaira VE, Cassidy C, Kus L, Gong S, Jankowski MP, Luo W, Heintz N, Koerber HR, Woodbury CJ, Ginty DD (2011) The functional organization of cutaneous low-threshold mechanosensory neurons. *Cell* 147:1615–1627.
- Liljencrantz J, Björnsdotter M, Morrison I, Bergstrand S, Ceko M, Seminowicz D a, Cole J, Bushnell MC, Olausson H (2013) Altered C-tactile processing in human dynamic tactile allodynia. *Pain* 154:227–234.
- Lindeberg J, Usoskin D, Bengtsson H, Gustafsson A, Kylberg A, Söderström S, Ebendal T (2004) Transgenic expression of Cre recombinase from the tyrosine hydroxylase locus. *Genesis* 40:67–73.
- Liu Q, Vrontou S, Rice FL, Zylka MJ, Dong X, Anderson DJ (2007) Molecular genetic visualization of a rare subset of unmyelinated sensory neurons that may detect gentle touch. *Nature Neuroscience* 10:946–948.
- Löken LS, Wessberg J, Morrison I, McGlone F, Olausson H (2009) Coding of pleasant touch by unmyelinated afferents in humans. *Nature Neuroscience* 12:547–548.
- Lou S, Duan B, Vong L, Lowell BB, Ma Q (2013) Runx1 Controls Terminal Morphology and Mechanosensitivity of VGLUT3-expressing C-Mechanoreceptors. *Journal of Neuroscience* 33:870–882.
- Lu Y, Perl ER (2003) A specific inhibitory pathway between substantia gelatinosa neurons receiving direct C-fiber input. *The Journal of Neuroscience* 23:8752–8758.

- Malmberg A, Chen C, Tonegawa S, Basbaum A (1997) Preserved Acute Pain and Reduced Neuropathic Pain in Mice Lacking PKC $\gamma$ . *Science* 278:279–284.
- Matsushita N, Kobayashi K, Miyazaki JI, Kobayashi K (2004) Fate of transient catecholaminergic cell types revealed by site-specific recombination in transgenic mice. *Journal of Neuroscience Research* 78:7–15.
- Molliver DC, Radeke MJ, Feinstein SC, Snider WD (1995) Presence or absence of TrKA protein distinguishes subsets of small sensory neurons with unique cytochemical characteristics and dorsal horn projections. *Journal of Comparative Neurology* 361:404–416.
- Mori M, Kose A, Tsujino T, Tanaka C (1990) Immunocytochemical localization of protein kinase C subspecies in the rat spinal cord: light and electron microscopic study. *The Journal of Comparative Neurology* 299:167–177.
- Murakami T, Kanchiku T, Suzuki H, Imajo Y, Yoshida Y, Nomura H, Cui D, Ishikawa T, Ikeda E, Taguchi T (2013) Anti-interleukin-6 receptor antibody reduces neuropathic pain following spinal cord injury in mice. *Experimental and Therapeutic Medicine* 6:1194–1198.
- Nordin M (1990) Low-threshold Mechanosensitive and Nociceptive Units with Unmyelinated (C) Fibers in the Supraorbital Nerve. *The Journal of Physiology* 426:229–240.
- Oatway MA, Chen Y, Weaver LC (2004) The 5-HT<sub>3</sub> receptor facilitates allodynia following spinal cord injury. *Pain* 110:259–268.
- Olausson H, Lamarque Y, Backlund H, Morin C, Wallin BG, Starck G, Ekholm S, Strigo I, Worsley K, Vallbo AB, Bushnell MC (2002) Unmyelinated tactile afferents signal touch and project to insular cortex. *Nature Neuroscience* 5:900–904.
- Peirs C, Patil S, Bouali-Benazzouz R, Artola A, Landry M, Dallel R (2014) Protein Kinase C gamma Interneurons in the Rat Medullary Dorsal Horn: Distribution and Synaptic Inputs To These Neurons, and Subcellular Localization of the Enzyme. *Journal of Comparative Neurology* 522:393–413.
- Peirs C, Seal RP (2016) Neural circuits for pain: Recent advances and current views. *Science (New York, NY)* 354:578–584.
- Pitcher M., Le Pichon C.E., Chesler A. (2016) Functional Properties of C-Low Threshold Mechanoreceptors (C-LTMRs) in Nonhuman Mammals. In: Olausson H., Wessberg J., Morrison I., McGlone F. (eds) *Affective Touch and the Neurophysiology of CT Afferents*. Springer, New York, NY
- Rasmussen PV, Sindrup SH, Jensen TS, Bach FW (2004) Symptoms and signs in patients with suspected neuropathic pain. *Pain* 110:461–469.
- Savitt JM, Jang SS, Mu W, Dawson VL, Dawson TM (2005) Bcl-x Is Required for Proper Development of the Mouse Substantia Nigra. *Journal of Neuroscience* 25:6721–6728.
- Schotzinger R, Landis S (1990) Postnatal development of autonomic and sensory innervation of thoracic hairy skin in the rat. *Cell and Tissue Research* 260:575–587.

- Seal R, Wang X, Guan Y, Raja S, Woodbury CJ, Basbaum A, Edwards RH (2009) Injury-induced mechanical hypersensitivity requires C-low threshold mechanoreceptors. *Nature* 462:651–655.
- Segatore M (1994) Understanding chronic pain after spinal cord injury. *The Journal of Neuroscience Nursing* 26(4):230-236.
- Shields SD, Ahn H-S, Yang Y, Han C, Seal RP, Wood JN, Waxman SG, Dib-Hajj SD (2012) Nav1.8 expression is not restricted to nociceptors in mouse peripheral nervous system. *Pain* 153:2017–2030.
- Siddall PJ, McClelland JM, Rutkowski SB, Cousins MJ (2003) A longitudinal study of the prevalence and characteristics of pain in the first 5 years following spinal cord injury. *Pain* 103:249–257.
- Tie-Jun SS, Xu Z, Hökfelt T (2001) The expression of calcitonin gene-related peptide in dorsal horn neurons of the mouse lumbar spinal cord. *Neuroreport* 12:739–743.
- Tom Tang Y, Emtage P, Funk WD, Hu T, Arterburn M, Park EEJ, Rupp F (2004) Tafa: A novel secreted family with conserved cysteine residues and restricted expression in the brain. *Genomics* 83:727–734.
- Usoskin D, Furlan A, Islam S, Abdo H, Lönnerberg P, Lou D, Hjerling-Leffler J, Haeggström J, Kharchenko O, Kharchenko P V., Linnarsson S, Ernfors P (2015) Unbiased classification of sensory neuron types by large-scale single-cell RNA sequencing. *Nature Neuroscience* 18:145–153.
- Vallbo Å, Olausson H, Wessberg J (1999) Unmyelinated Afferents Constitute a Second System Coding Tactile Stimuli of the Human Hairy Skin. *Journal of Neurophysiology* 81:2753–2763.
- von Euler US (1971) Adrenergic neurotransmitter functions. *Science (New York, NY)* 173:202–206.
- Vrontou S, Wong AM, Rau KK, Koerber HR, Anderson DJ (2013) Genetic identification of C fibres that detect massage-like stroking of hairy skin in vivo. *Nature* 493:669–673.
- Watson JL, Hala TJ, Putatunda R, Sannie D, Lepore AC (2014) Persistent at-level thermal hyperalgesia and tactile allodynia accompany chronic neuronal and astrocyte activation in superficial dorsal horn following mouse cervical contusion spinal cord injury. *PLoS One* 9:e109099.
- Yeziarski RP, Yu CG, Mantyh PW, Vierck CJ, Lappi DA (2004) Spinal neurons involved in the generation of at-level pain following spinal injury in the rat. *Neuroscience Letters* 361:232-236.
- Zhang Y, Jiang X, Snutch TP, Tao J (2013) Modulation of low-voltage-activated T-type Ca<sup>2+</sup> channels. *Biochimica et Biophysica Acta - Biomembranes* 1828:1550–1559.

Zhu YF, Wu Q, Henry JL (2012) Changes in functional properties of A-type but not C-type sensory neurons in vivo in a rat model of peripheral neuropathy. *Journal of Pain Research* 5:175–192.